Establishing the European Geological Surveys Research Area to deliver a Geological Service for Europe

Deliverable 3.2 + 4.2

PILOT DESCRIPTION AND ASSESSMENT

The Netherlands
&
De Raam, Netherlands

Authors and affiliation:

Willem J. Zaadnoordijk (TNO-GSN)
Timo Kroon (Deltares)
Eva Schoonderwoerd (Deltares)
Janneke Pouwels (Deltares)

This report is part of a project that has received funding by the European Union's Horizon 2020 research and innovation programme under grant agreement number 731166.

Deliverable Data	
Deliverable number	D3.2, D4.2
Dissemination level	Public
Deliverable name	Pilot description and assessment
Work package	WP3, WP4
Lead WP/Deliverable beneficiary	GEUS
Deliverable status	
Version	3
Date	26/03/2021

LIST OF ABBREVIATIONS & ACRONYMS

AHN	Open Source Data set with Actual Elevation Levels for the Netherlands (in Dutch “Actueel Hoogtebestand Nederland”)
BIS	Data base with Dutch soil characteristics (in Dutch: “Bodemkundig Informatie Systeem”).
Deltares	Dutch research institute.
iMOD	Open Source modelling software of Deltares, based on the MODFLOW model (USGS), adapted to apply for large datasets, and including a user interface.
LGN	Data set with land use for the Netherlands (in Dutch: ”Landelijk Grondgebruik Nederland”)
Metran	Tool for transfer noise modelling and dynamic factor analysis of groundwater head time series.
NAP	National Dutch Datum (equal to mean sea level; in Dutch: “Normaal Amsterdams Peil”)
NHI	Netherlands Hydrological Instrument (integrated hydrological model based on iMOD).
NHI-LHM	National Hydrological Model of the NHI (in Dutch: “Landelijk Hydrologisch Model”).
TNO-GSN	TNO Geological Survey of the Netherlands.

TABLE OF CONTENTS

LIST OF ABBREVIATIONS & ACRONYMS 5

1 EXECUTIVE SUMMARY 5

2 INTRODUCTION 8

3 PILOT AREAS 11
- 3.1 Site description and data 11
  - 3.1.1 Meteorological data 11
  - 3.1.2 Topography 13
  - 3.1.3 Geology/Aquifer type 14
  - 3.1.4 Soil types 15
  - 3.1.5 Surface water bodies 16
  - 3.1.6 Land use 17
  - 3.1.7 Abstractions/irrigation 19
- 3.2 Climate change challenge 20
  - 3.2.1 How is the climate expected to change in the Netherlands 20
  - 3.2.2 What are the challenges related to the expected climate change? 21

4 METHODOLOGY 22
- 4.1 National Hydrological Model NHI-LHM 22
  - 4.1.1 NHI components and coupling 23
  - 4.1.2 NHI-LHM version and calibration 24
- 4.2 Regional groundwater model used in de pilot Raam 24
- 4.3 Metran 25
- 4.4 Climate change scenarios 26
  - 4.4.1 TACTIC standard Climate Change scenarios 27

5 RESULTS 29
- 5.1 National pilot 29
  - 5.1.1 Reference period results 29
  - 5.1.2 Climate change scenario results 38
- 5.2 De Raam 50
  - 5.2.1 Reference period results 50
  - 5.2.2 Climate change scenario results 56

6 DISCUSSION 57
- 6.1 NHI-LHM 57
- 6.2 De Raam 58
- 6.3 Metran 59
- 6.4 Comparison between models 62
  - 6.4.1 Regional and national physically based distributed models 62
  - 6.4.2 Physically based distributed models and time series models 65

7 CONCLUDING REMARKS 70

8 REFERENCES 71

1 EXECUTIVE SUMMARY

TNO Geological Survey of the Netherlands (TNO-GSN) and Deltares together contribute two pilots to the TACTIC project: a national pilot “Netherlands” and a regional pilot “de Raam”.

Pilot name	Netherlands	*Example of groundwater recharge (mm/year) calculated with NHI-LHM (average 1996-2008)* 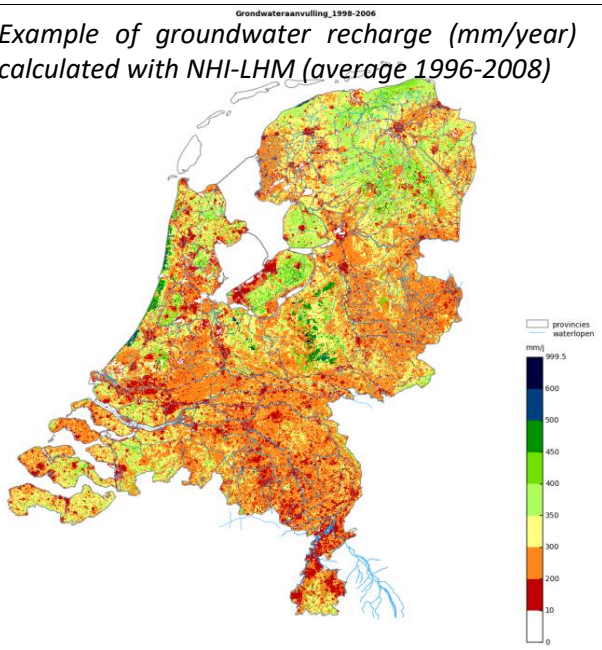
Country	Netherlands	
EU-region	North-western Europe	
Area (km^2)	40 500	
Aquifer geology and type classification	Sand and gravel – Porous; Chalk – Fissured	
Primary water usage	Drinking water / Irrigation / Industry / Ecology	
Main climate change issues	Climate change (change of precipitation, evaporation, incoming river discharges and sea level rise), combined with socio-economic developments	
Models and methods used	Integrated Hydrological model (national application of the Netherlands Hydrological Instrument; NHI-LHM), Time series analysis (using Metran)	
Key stakeholders	Rijkswaterstaat, Ministry of Infrastructure and Water (including Delta Programme), Ministry of Economic Affairs and Climate policy. Further the waterboards, provinces and drinking water companies are involved in development and application of the hydrologic instrument.	
Contact persons	Timo Kroon, Deltares, timo.kroon@deltares.nl Willem Jan Zaadnoordijk, TNO, willem_jan.zaadnoordijk@tno.nl	

This pilot considers the groundwater and interaction with the surface water system at a national scale with the national hydrologic model for the Netherlands (NHI-LHM). Usually this integrated model for simulations in the subsurface and surface water in the Netherlands is applied for national water management and national policy making (quantity and water quality). Water management on a national level with the model relates to national water supply and measures for drought prevention, such as setting of the weirs in the main water system in the (branches of) the Meuse and Rhine, and the management of the storage in lake IJsselmeer, which serves during drought as the largest fresh water reservoir in the Netherlands.

Within TACTIC simulations with the national model are presented for the current climate and for four climate change scenarios. The calculated heads are compared at a few locations with simulations from linear transfer noise models (created using Metran, the groundwater dynamics tool of http://www.grondwatertools.nl).

Pilot name	De Raam	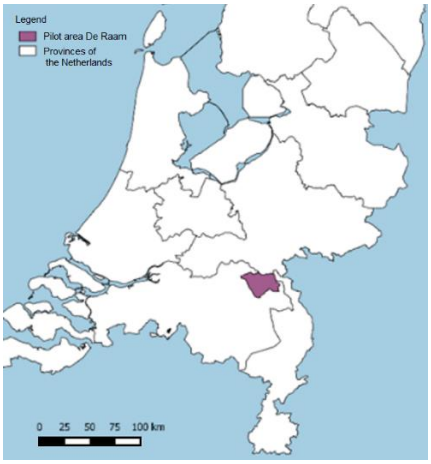
Country	Netherlands	
EU-region	North-western Europe	
Area (km^2)	224	
Aquifer geology and type classification	Sand and gravel – Porous	
Primary water usage	Irrigation / Ecology / Drinking water	
Main climate change issues	climate change (change of precipitation, evaporation, incoming river discharges and sea level rise), combined with socio-economic developments	
Models and methods used	Integrated Hydrological model (regional model, based on iMOD), Time series analysis (using Metran)	
Key stakeholders	Waterboard Aa en Maas, province of Noord-Brabant and drinking water company Brabant Water	
Contact person	Timo Kroon, Deltares, timo.kroon@deltares.nl Willem Jan Zaadnoordijk, TNO, willem_jan.zaadnoordijk@tno.nl	

For the regional pilot in the Netherlands, 'de Raam' a regional model is applied. This model has been developed for regional management of groundwater and surface water and is a refined version of the national instrument (NHI). It is used by the waterboard, province and drinking water company to investigate the effects of regional and local measures in the current and future (climate change) situation.

Within TACTIC the regional groundwater model has been used to simulate the current climate and for the TACTIC climate change scenarios. A comparison between the results from the regional and the national integrated hydrological model is presented.

At the location of a few monitoring wells, the calculated heads are compared with simulations from linear transfer noise models from Metran. Also time series modelling has been carried out for a few piezometers influenced by an accident on the river Meuse during which the river level was 3 meters lower than normal.

The transfer noise modelling of monitoring of measured groundwater heads reproduces the measured heads better than a distributed physically based model at the location of the piezometer. However, a physically based model is better suited for scenario calculations, even if the scenarios only involve changes in the explaining variables of the transfer noise model. The reason for this, is the non-linearity of the groundwater system or change of system behaviour when the situation differs from the calibration period. The simulations of time series near the river Meuse illustrated this with different responses to the river level for the normal situation and during an accident with much lover water levels.

The transfer noise models using only groundwater heads as calibration variables do not provide a useful estimate of groundwater recharge. Moreover, transfer noise modelling of time series itself does not provide information in between piezometers – for the best spatial estimation of historic groundwater heads a combination of time series and a physically based distributed model provides the best results.

Lastly, a comparison of a fine resolution regional model and a coarse resolution national model indicates that the fine resolution is necessary to study local variations. This also corresponds to the different purposes of these models. The national model is used for the management of the main rivers and for national policy development. The model for De Raam is intended for improving the regional water management, e.g. by evaluating concrete local measures.

2 INTRODUCTION

The Netherlands is bordered by Belgium, Germany and the North Sea. The land area is 40 500 km^2. The surface topography is relatively flat ranging from below sea level in polders in the Western and Northern parts to 300 meters above in the South-eastern corner.

The large scale differences in the elevation of the phreatic groundwater level are related to the net groundwater replenishment from precipitation areas with relatively little drainage and surface water in the higher mostly Pleistocene inland part of the country and the drainage in polders and other lower areas mostly with a Holocene cover. The drainage is strongly influenced by anthropogenic surface waters.

The fresh groundwater of meteoric origin in this system in the Netherlands reaches its largest depths in the Holocene coastal dunes (tens of metres depth), the Pleistocene ice-pushed hills (Veluwe and Utrechtse Heuvelrug) in the central and Eastern part of the country (up to few hundred metres depth), and in the supra-regional groundwater flow system in the South-eastern part of the country (≥ 600 m). These fresh parts of the groundwater flow systems occur in unconsolidated sedimentary sequences of dominantly Holocene and Pleistocene to Neogene age.

The availability of groundwater in the Netherlands is influenced by the surface waters. Surface water is mainly supplied from the catchment areas of the Rhine and the Meuse (see figure 2.1).

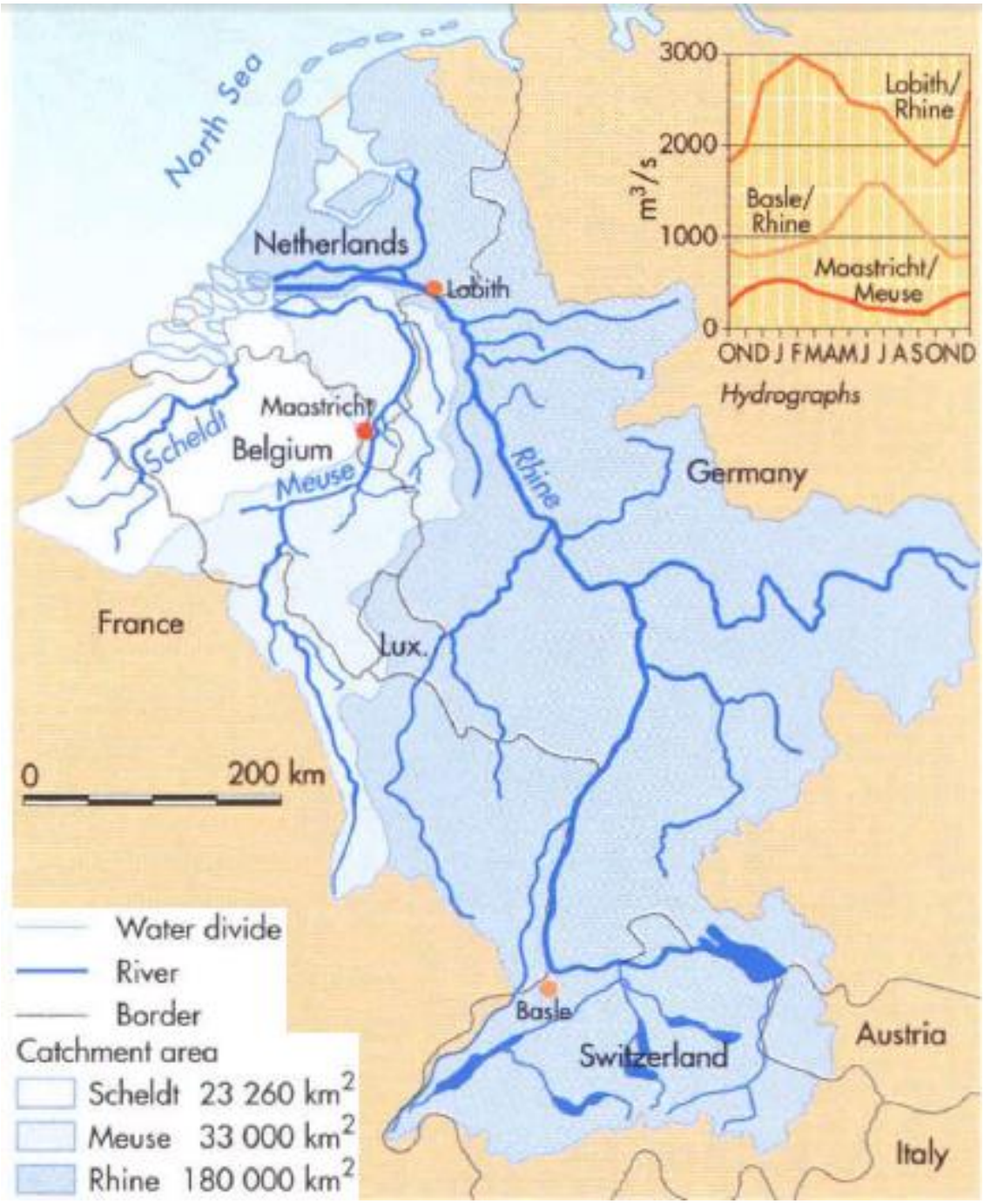

Figure 2.1 The Netherlands situated in the catchment of the river Rhine and Meuse

Deltares and TNO Geological Survey of the Netherlands contribute two pilots to the TACTIC project: a national and a regional pilot. For both pilots, two types of models are applied:

- Integrated hydrological model;
- Time series model.

The integrated models are based on the Netherlands Hydrological Instrument, NHI (de Lange et al., 2014). The time series models have been created using Metran (Berendrecht & van Geer, 2016).

The Netherlands Hydrological Instrument (NHI) (https://www.nhi.nu) is used for integrated hydrological modelling. It contains data and software for both the surface water and groundwater, based on iMOD (Vermeulen et al, 2020). The nationwide modelling is carried out with the LHM (National Hydrological Model) (Janssen et al., 2020), but the NHI also contains several regional models.

Metran is a tool for transfer noise modelling of groundwater head time series (Berendrecht & van Geer, 2016). It is applied to the groundwater head time series in the Dutch national subsurface database (https://www.dinoloket.nl/en/subsurface-data) on the groundwater tools website http://www.grondwaterstandeninbeeld.nl (Zaadnoordijk et al., 2019).

The National pilot of the Netherlands focusses on the groundwater simulations and interaction with the surface water at a national scale, based on 250 m grid cell calculations. On this scale the national hydrologic model (NHI-LHM) is typically applied in national policy studies in the Netherlands, for example to explore the effects of measures and climate change on the water quantity or water quality (salinity or nutrients). On this scale the model is also applied for national water management during drought, to decide on possible measure, for example concerning the weirs in the main water system in the (branches of) the Meuse and Rhine, and the management of the storage in lake IJsselmeer, which serves during drought as large fresh water reservoir in the Netherlands.

The regional pilot in the Netherlands, 'de Raam', uses a regional model of NHI (the GRoundwater model of waterboard Aa en Maas, 'GRAM', Deltares & Aa en Maas, 2020), which has been developed for regional water management. The concepts and data are based on the same instrument (NHI) as the national model, but the model is applied with extra and more detailed information and on a higher resolution, typically on 25 m grid cell basis. This model is used in several projects for regional water management, for example to decide on measures in the regional water system, to explore the effects of land use (mostly agricultural and natural) and the regional effects of climate change on the regional groundwater and surface water system.

3 PILOT AREAS

3.1 Site description and data

Two pilot areas will be explained in this chapter: The Netherlands and The Raam. The Raam is a catchment area of the stream with the same name, situated in the province of Noord-Brabant. Figure 3.1 shows the location of The Raam within the Netherlands.

Figure 3.1 The location of pilot area The Raam within the Netherlands.

Data needed for physically-based distributed groundwater modelling are available as open data via the NHI data portal (https://data.nhi.nu/) and additional data sources within the Netherlands:

- Meteorological data is available from the Royal Dutch Meteorological Institute KNMI (http://www.knmi.nl/nederland-nu/klimatologie-metingen-en-waarnemingen),
- Data about the large surface waters from Rijkswaterstaat (http://waterinfo.rws.nl)
- Subsurface data including groundwater head measurements are available via TNO Geological Survey of the Netherlands (https://www.DINOloket.nl).
- Soil data: http://www.bodemdata.nl/

3.1.1 Meteorological data

According to the Köppen system, the Netherlands has a temperate maritime climate (type Cfb) with relatively mild winters, mild summers and rainfall throughout the year. The precipitation of 890 mm per year (climate period 1981-2010) is quite evenly distributed throughout the year, see table 3.1. The evaporation is on average 540 mm per year.

Figure 3.2 shows the spatial distribution of the precipitation and evaporation in the Netherlands. Higher precipitation can be found in some Eastern parts in the North, middle and South of the country, as well as some polder areas in the Western part of the country. The Southwest of the Netherlands has the highest evaporation, with a decrease in evaporation in the North-eastern direction.

Meteorological time series are available from 35 weather stations (hourly and daily precipitation and evaporation) and about 300 precipitation stations (daily precipitation) in the Netherlands. Those data are used in the ground water modelling.

Table 3-1 Monthly precipitation in the Netherlands, averaged over 1981 – 2010 (Bot, 2016).

Month	Average precipitation [mm]
January	75
February	59
March	74
April	45
May	65
June	68
July	84
August	77
September	81
October	89
November	96
December	84

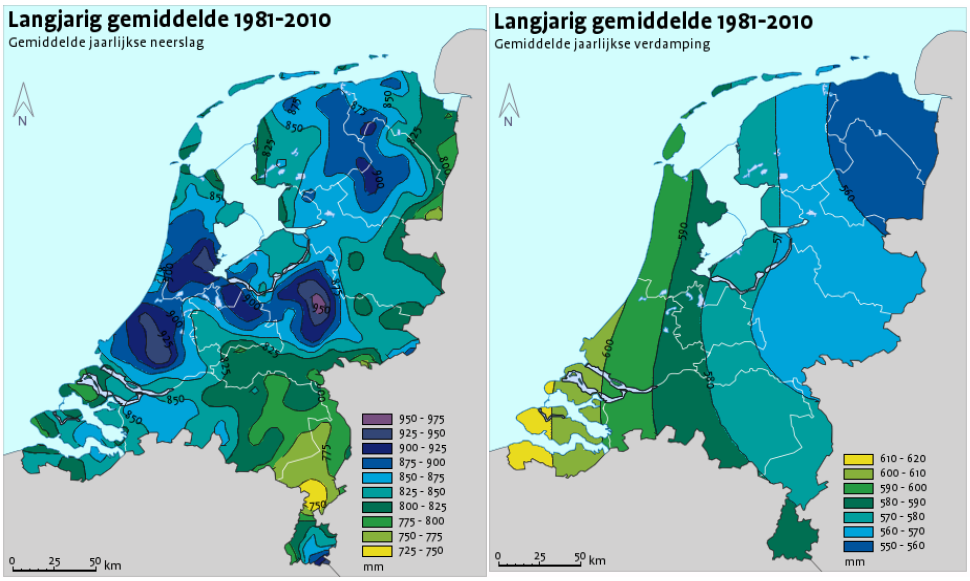

Figure 3.2 The average precipitation (left) and evaporation (right) for the period 1981 – 2010 in the Netherlands (KNMI, 2011).

3.1.2 Topography

Figure 3.3 shows the surface elevation of the Netherlands, based on public data for the Netherlands (AHN). Part of the Netherlands is below sea level; the lowest level is 6.7 m below mean sea level. In the South and East, the height of the landscape is relatively high. The maximum elevation in the central area of the Netherlands is about 100 meters above mean sea level; in the Southeast the highest elevation is 322 meters above mean sea level.

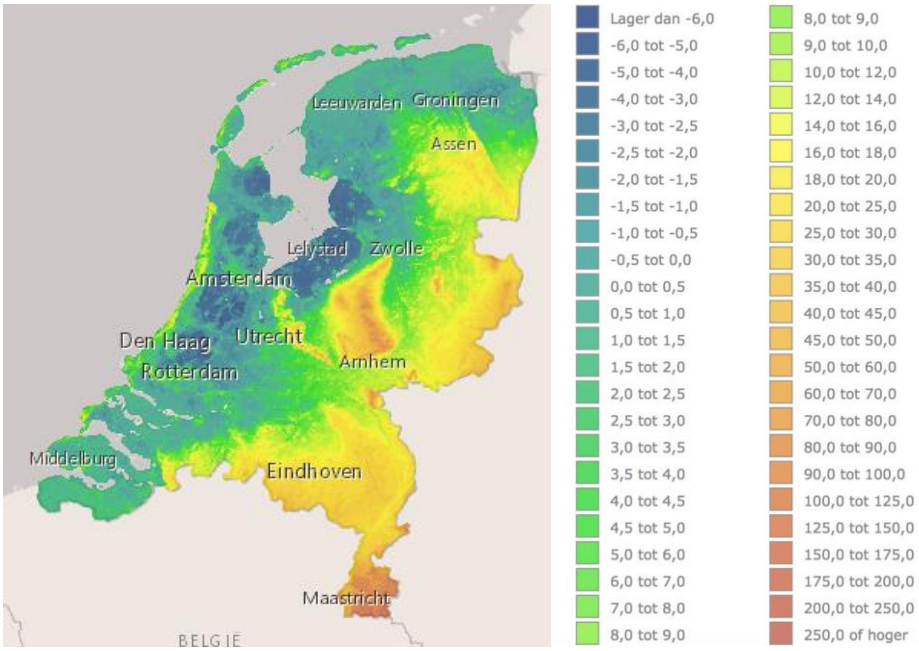

Figure 3.3 Surface elevation of the Netherlands, in meter above mean sea level (m+ NAP). Source: https://www.ahn.nl.

Figure 3.4 shows the surface elevation in the pilot area of De Raam (located between the cities of Arnhem and Eindhoven shown in Figure 3.3).

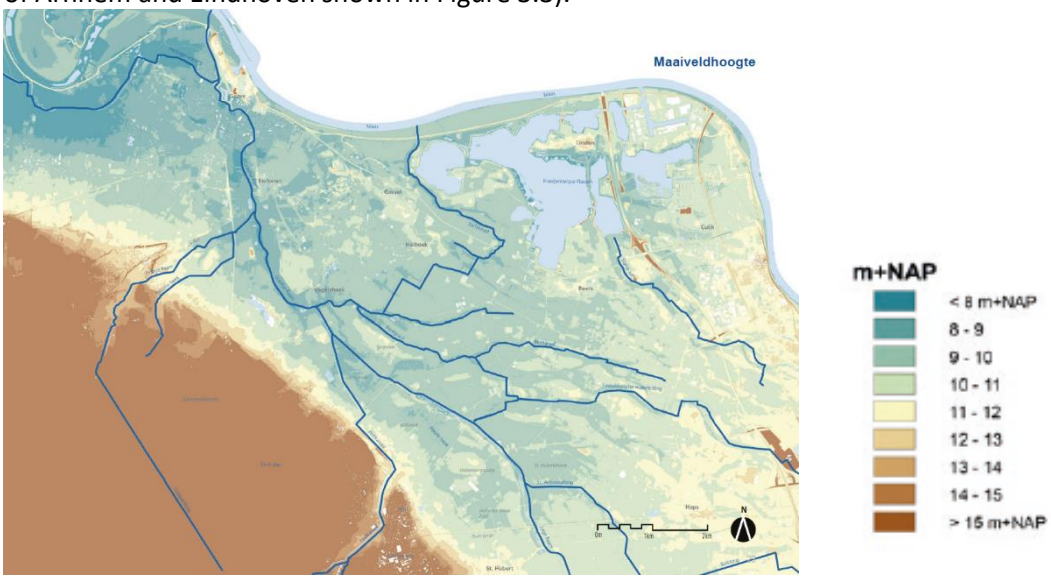

Figure 3.4 Surface elevation (m+NAP) of the area "De Raam" (Besselink, 2018).

3.1.3 Geology/Aquifer type

The Netherlands is located in the North Sea basin. Groundwater resources are limited primarily mainly to deposits of Quaternary age, which are the result of the interplay of rivers (Rhine, Meuse, Scheldt, and the previous Baltic river system Eridanos) and the North Sea.

Figure 3.5 gives a hydrogeological section across the country. It shows the Holocene confining layer, which is present in the Western and Northern parts of the country, the ice pushed ridges in the centre, and the clayey units of the marine Formations of Maassluis (MSk), Oosterhout (Ook), and Breda (BRk) which usually act as hydrological base depending on the location and context.

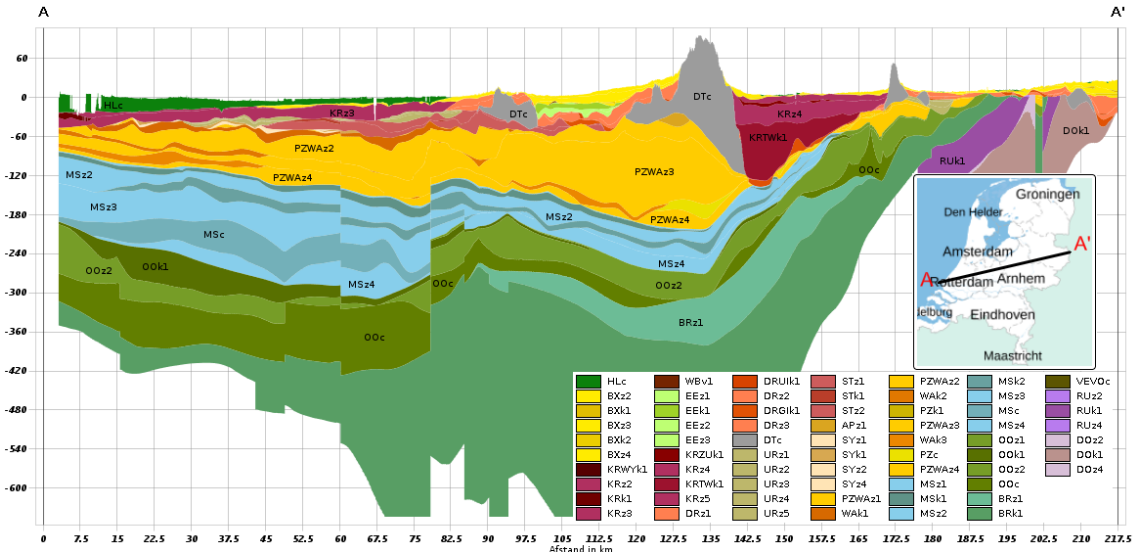

Figure 3.5 Hydrogeological units of the regional hydrogeological model REGIS II (see https://www.dinoloket.nl/en/subsurface-models) with the last two characters indicating sandy (z), clayey (k), or complex (c) units within the geological units.

The sandy units of the Formations of Kreftenheye and Peize & Waalre are important aquifers. Background information on the geological units can be found in the online stratigraphic nomenclator: https://www.dinoloket.nl/en/stratigraphic-nomenclature.

The South-eastern corner of the Netherlands has the highest elevations and also the subsurface is different from the rest of the country (Figure 3.6 and figure 3.3). There is a cover of loss and older geologic units come close to the surface, notably the chalk aquifers of the Formations of Gulpen (GUq), Maastricht (MTq), and Houthem (HOq).

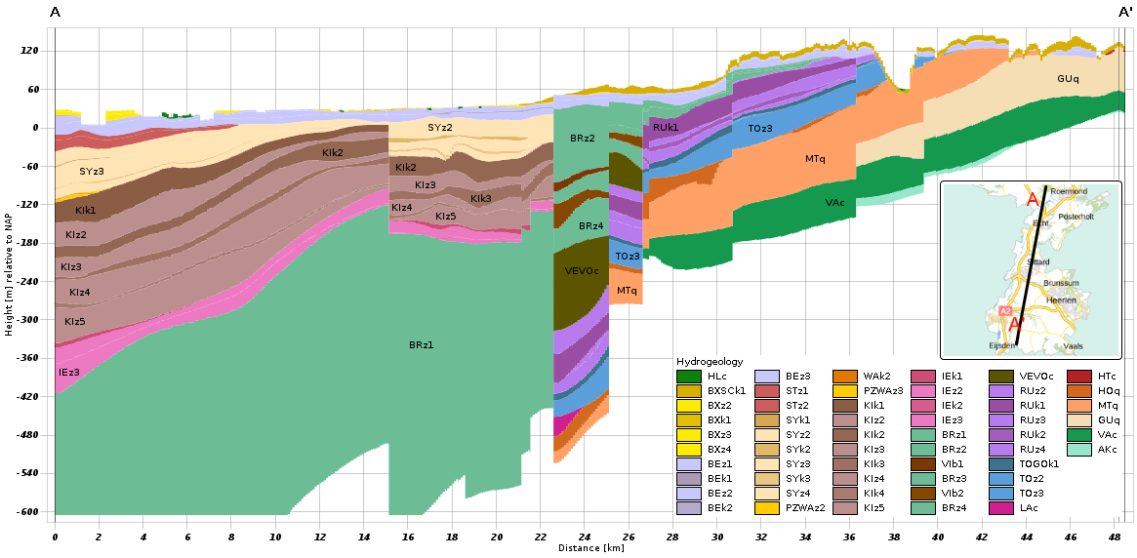

Figure 3.6 REGIS II section in South-eastern corner of the Netherlands with the highest elevation and the oldest deposits of the Netherlands.

3.1.4 Soil types

Figure 3.7 shows a soil map of the Netherlands, based on BIS (the Dutch Soil Database). The sandy soils occur in the South and East of the country. Along the main rivers, in the Southwest and in the North of the Netherlands, clayey soils can be found. The purple areas have peat soils and in the South-eastern corner, loamy soils occur. In the Raam area clayey soils can be found near the river Meuse in the North, and sandy soils in the South.

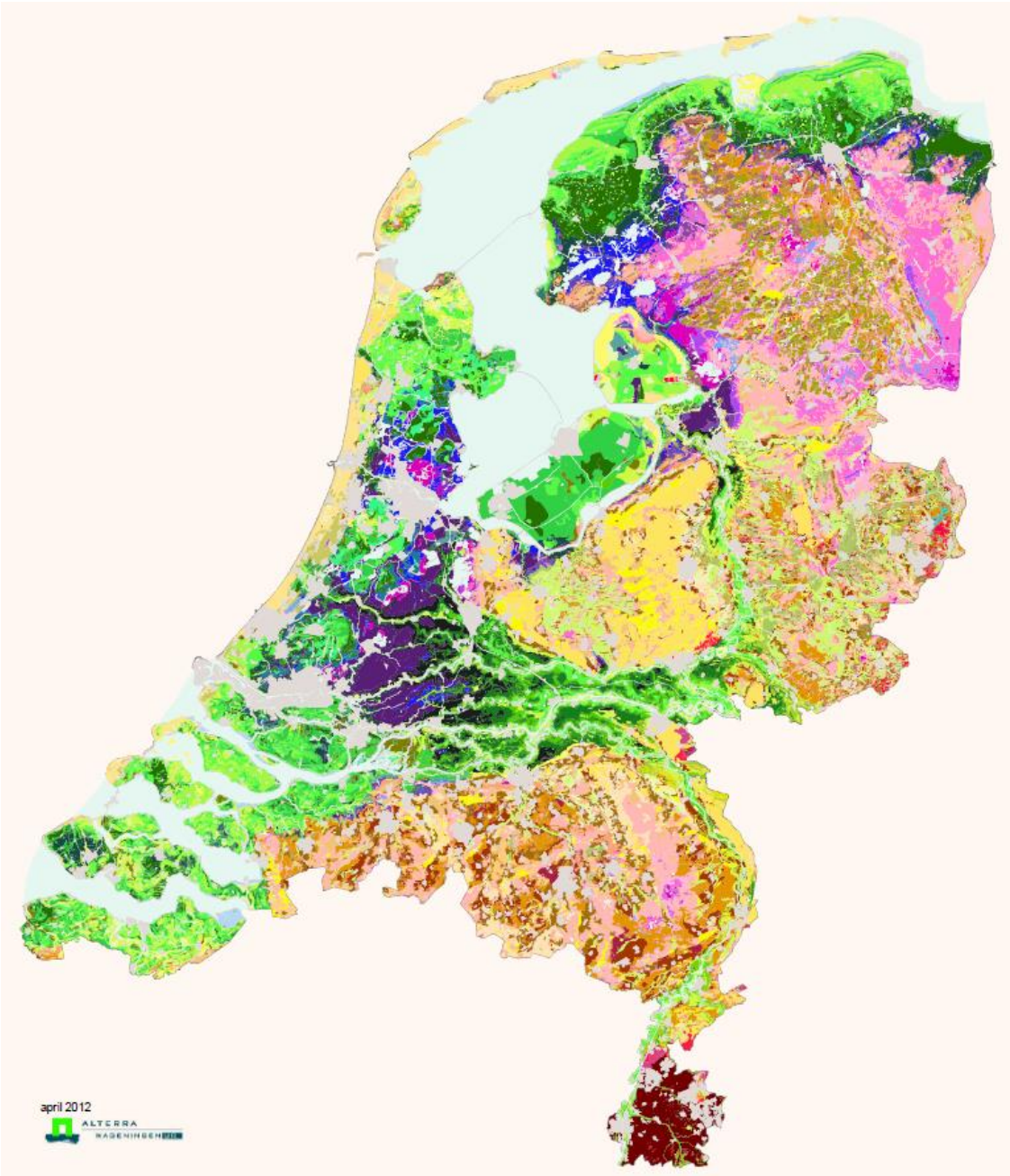

Figure 3.7 Soil types of the Netherlands (Wosten et al., 2012). The purple/blue colours are peat soils, the yellow/brown colours are sandy soils and green colours are clay soils. The dark brown colour in the South-eastern corner are loamy soils.

3.1.5 Surface water bodies

Figure 3.8 shows the largest surface water bodies in the Netherlands, including the larger river systems coming in from the East (Rhine) and Southeast (Meuse) (see also figure 2.1). The Scheldt flows from Belgium into an estuary in the Southwest. In the central West and North of the Netherlands lakes can be found, which are the result of peat extractions in the past. A larger zone in the North and the West of the country have many smaller water courses and ditches,

mainly in the lower areas (see *Figure 3.3*) with clay and peat soils (see *Figure 3.7*). These water bodies have a controlled surface water level and strongly influence the phreatic groundwater level, often in combination with tube drainage. This way inundation is prevented in winter and for the polders with large upward seepage also in summer. The surface water system serves as a water supply system in times of drought. In the sandy areas in the East and the South, less water bodies are present and these do not provide water in times of drought. These regions are more dependent on precipitation and irrigation from groundwater.

Figure 3.8 Surface water bodies (Topografische Dienst Kadaster, 2019)

3.1.6 Land use

Figure 3.9 shows the different types of land use in the Netherlands. A large part of the area in the Netherlands is used for agriculture. Urban area is most concentrated in the central Western part, whereas in the Eastern part larger areas with forest and dry nature occur.

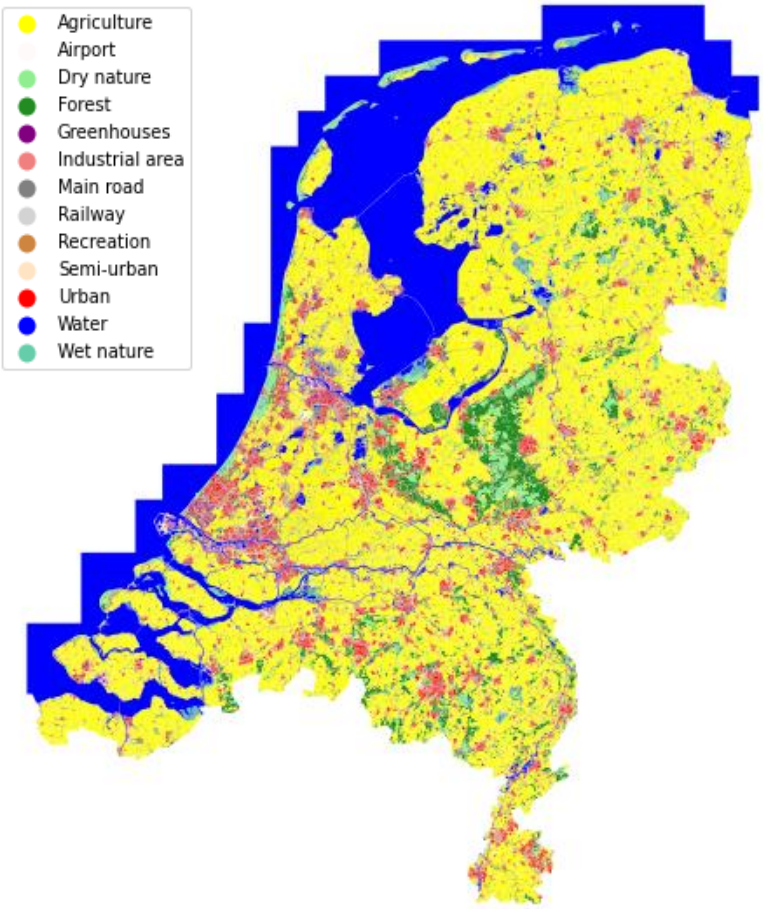

Figure 3.9. Land use types in the Netherlands (source: Dutch Statistical Bureau, CBS).

Figure 3.10 shows the different types of land use in De Raam, where mostly agricultural land can be found. Also, some urban areas and forests occur. The lakes in the Northeast are connected to the river Meuse, which is the North-eastern boundary of the area of De Raam.

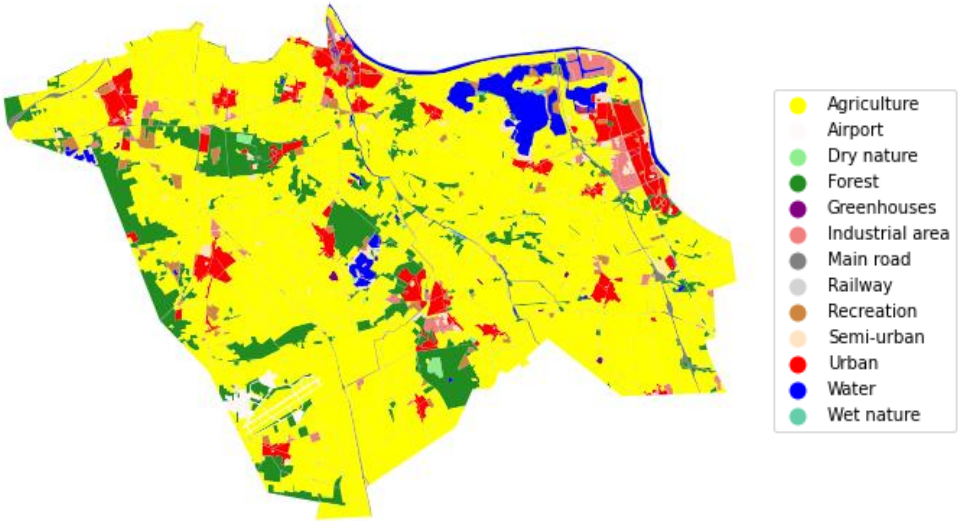

Figure 3.10 Land use types in the pilot De Raam

3.1.7 Abstractions/irrigation

Groundwater abstraction occurs in the Netherlands for drinking water production, industry and agriculture (for livestock and (overhead) irrigation). *Figure 3.11* shows the wells fields used for drinking water production. They are located in areas with fresh water aquifers, which mostly coincide with higher surface elevations (cf. *Figure 3.3*).

Figure 3.11: Blue dots indicate well fields for drinking water supply, yellow is groundwater extraction at the riverbank, orange are water infiltration locations, green is drinking water supply from surface water and red are emergency wells. The different areas indicate the regions of the drinking water supply companies (Vewin, 2017).

Figure 3.12 shows the locations of irrigation wells together with the locations where surface water is used for irrigation.

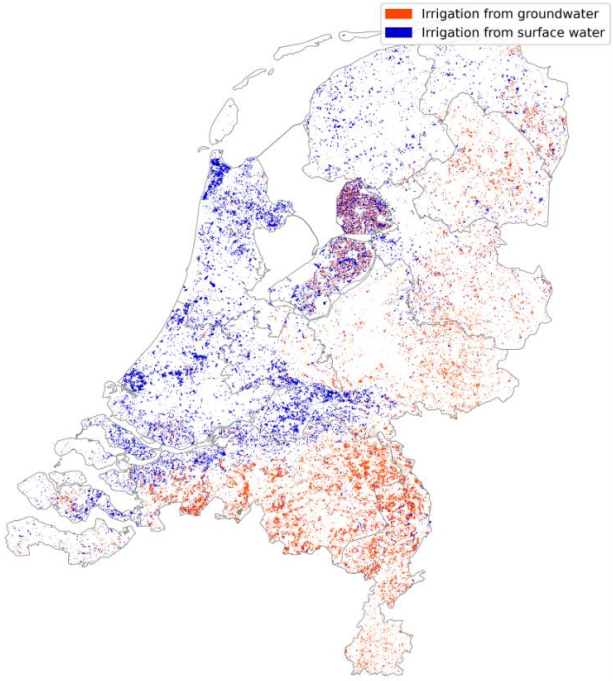

Figure 3.12: Locations of irrigation wells and irrigation from surface water (data available at https://www.nhi.nu).

3.2 Climate change challenge

3.2.1 How is the climate expected to change in the Netherlands

The Royal Dutch Meteorological Institute prepares climate change scenarios for the Netherlands. According to the most recent scenarios, climate change is expected to cause the following effects in the Netherlands (KNMI, 2015):

- Temperature will rise;
- Mild winters and hot summers will occur more often;
- Precipitation and extreme precipitation in the winter will increase;
- The intensity of extreme summer precipitation will increase;
- Hail and thunder will become more intense;
- Changes in wind speed are small;
- The amount of foggy days will decrease.

These predicted effects are aligned with the European Environment Agency map that describes the expected climate change across the different areas in Europe as shown in *Figure 3.13*. Scenarios for future climate change in the Netherlands are described by KNMI (KleinTank et al., 2015). In those scenarios the most likely changes in the Netherlands are described according to the latest insights.

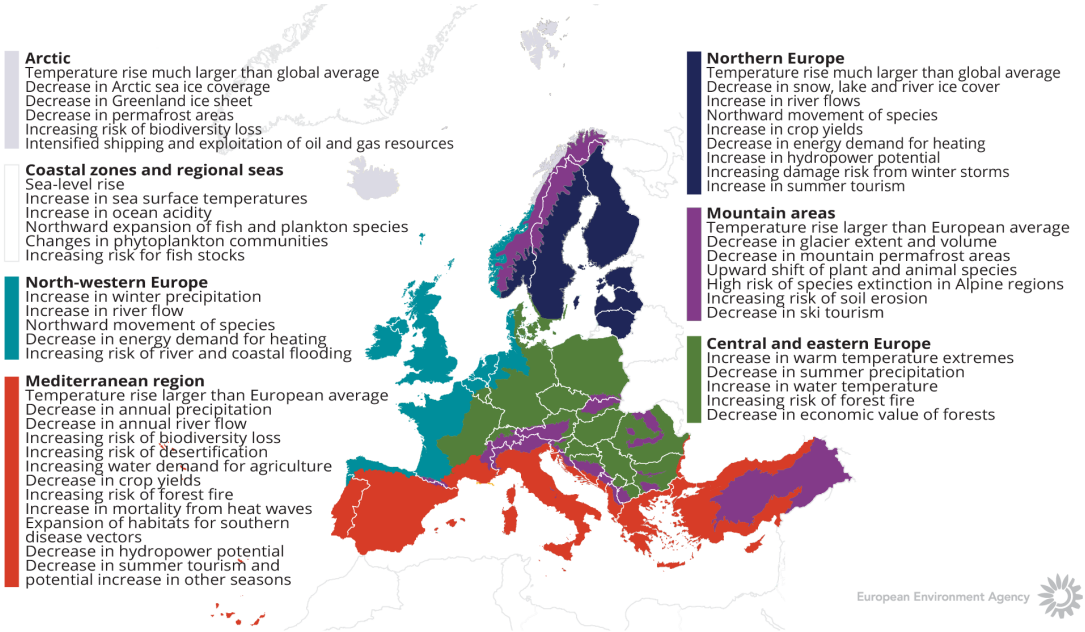

Figure 3.13. How is climate expected to change in Europe. The European Environment Agency map

3.2.2 What are the challenges related to the expected climate change?

Water shortage is one of the challenges from the extended droughts expected to result from climate change. This impacts many sectors, such as agriculture, ecology, and drinking water production, industrial water use, electricity production (because of restriction for cooling water), and transport (because of reduced depth of the rivers which are main waterways for shipping). Degradation of peat and emission of greenhouse gases threatens the peat areas (see *Figure 3.7*). In the Netherlands, lowering of the groundwater table in historical cities poses a special risk, because of wooden foundations of buildings that decay when they are no longer below the groundwater table.

Another major challenge is extreme precipitation, which can cause flooding. The threat from flooding is most severe in urban areas, where it is likely to be caused directly by precipitation. Streets can be covered by water, the ground floor of buildings may be flooded, and water can flow into basements. In addition, the sewer system may be overloaded, leading to sewage spilling into the surface water and causing water quality problems.

Sea level rise makes the coastal area more vulnerable for floods, and rivers more vulnerable for sea water intrusion.

4 METHODOLOGY

4.1 National Hydrological Model NHI-LHM

In 2005, Dutch national research institutes and the water authorities (both national and regional) started to combine their water expertise and financial means to construct a national water model: the Netherlands Hydrological Instrument NHI (https://www.nhi.nu). This had to replace various separated, partially parallel modelling efforts, such as the national models NAGROM (de Lange, 1991) and LGM (Lieste et al., 1993), and the regional model GMN (Iwaco, 1992). It started by bringing together the available data and technologies, resulting in a first version of the national model in 2008. In 2013, a next main version of NHI was achieved, based on the consensus of all national and regional water management organizations. An extensive description of the NHI can be found in De Lange et al. (2014).

The nationwide modelling is carried out with the LHM (National Hydrological Model), but the NHI also contains several regional models. The NHI contains a coupling of four sub-models, which together can simulate the groundwater, surface water and the vadose zone (see *Figure 4.1*). The groundwater is modelled with the use of iMOD (Vermeulen et al., 2020), which includes a Graphical User Interface developed by Deltares and an adapted version of MODFLOW 2005, to enable fast calculations in large domains. The surface water is divided into the regional surface water, modelled with the use of Mozart, and national surface water, which uses DM (Distribution Model) (De Lange et al, 2014). The vadose zone is modelled with the use of MetaSWAP (van Walsum et al., 2017). The grid cell size that is used in the NHI-LHM model is 250x250 m.

An important aim of the NHI is computing the water demand and allocation for different water users in periods of water scarcity. Therefore, the LHM is used within the National Water Model, a constellation of different models including water quality and effect modules for agriculture, terrestrial nature and other sectors. Besides, a special version of NHI is available for modelling salinity transport in the subsurface (Delsman et al, in prep 2021).

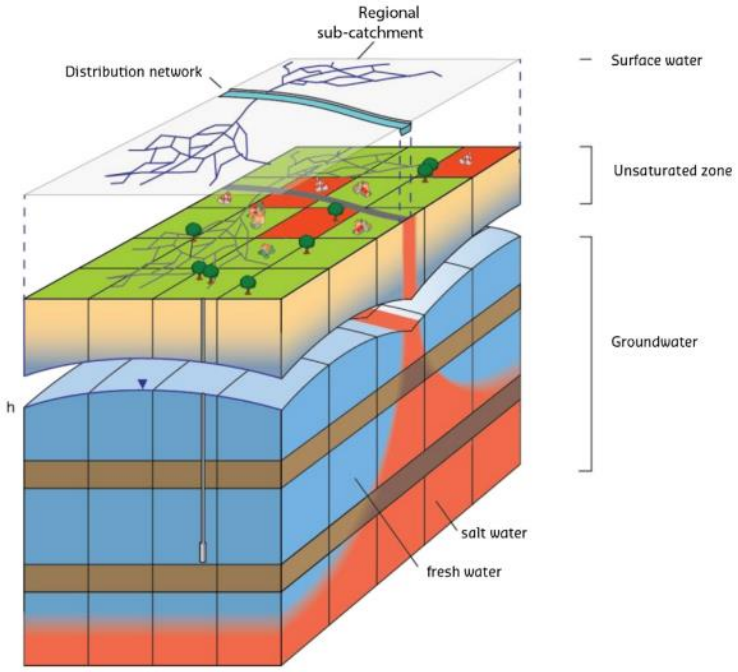

Figure 4.1 The hydrological components of the Netherlands Hydrological Instrument (NHI)

4.1.1 NHI components and coupling

The surface water is modelled on a large, national, scale with the Distribution Model (DM) and on local scale with Mozart. DM allocates water to various water users by optimizing the water demands. The allocation of water is calculated with water distribution rules, based on water management practice. This includes a prioritizing scheme for water scarcity, where first water is allocated to the most important category and then to the categories with lower priorities. These categories are as follows: 1: water safety (like dikes) or irreversible damage to nature areas. 2: public utilities (drinking water & energy). 3 & 4: for example agriculture, industry and recreation. MOZART is a lumped model, which calculates a balance for the surface water by accounting for withdrawals and discharges. MOZART is applied to every small catchment, resulting in a calculated surface water level that is coupled with the surface water levels in the corresponding MODFLOW cells.

The unsaturated zone is modelled with the use of MetaSWAP. This model computes the transfer of water between the saturated zone and the atmosphere, while also incorporating the root zone and vegetation. The coupling procedure is described by Van Walsum and Veldhuizen (2011). Recently the coupling procedure within NHI is improved by a BMI-coupling procedure, which is implemented in the original MODFLOW 6 code (Hughes et al., 2021, in prep.).

The groundwater, modelled with MODFLOW, interacts (drainage or infiltration) with the surface waters in MOZART. Other top system components in MODFLOW, the phreatic storage coefficient, phreatic head and the flux to and from the unsaturated zone, are based on information of MetaSWAP. Furthermore, the irrigation demand is calculated by MetaSWAP which results in a water demand for surface water in MOZART or groundwater in MODFLOW.

Recently, the national model has been extended with the crop growth model WOFOST (Hunink et al., 2019). This detailed crop model is coupled to MetaSWAP. By using WOFOST, the crop growth is not fixed input for the groundwater model, but calculated dynamically, depending on the condition in the soil and the atmosphere. This enables improved calculations of evapotranspiration, also for climate changes, because effect of changing temperatures and higher CO_2 concentrations on the crop growth can be taken into account.

The calculation of actual evapotranspiration of the crops within the combination MetaSWAP-WOFOST is based on Penman-Monteith, which is not directly compatible with the TACTIC climate scenarios with the delta change factors. Also, these scenarios do not contain carbon dioxide concentrations. This means that within the climate scenarios for TACTIC, the WOFOST option is not used.

4.1.2 NHI-LHM version and calibration

The national modelling is carried out with LHM version 4.1 (Janssen et al., 2020). The geohydrological schematization is represented by 8 model layers within NHI-LHM, based on geohydrological models of the Netherlands: REGIS II V2.2 (TNO-GSN, 2021a) and GeoTOP (TNO-GSN, 2020b).

NHI-LHM (version 4.1) has been calibrated in steady state mode using the average groundwater heads for the period 2011-2018 of piezometers available in the national subsurface database (https://www.dinoloket.nl/en/subsurface-data). The calibration was carried out by using the iPEST software, which an implementation in iMOD (Vermeulen et al., 2020) of the parameter estimation package PEST (Doherty, 2015). The calibrated parameters were the aquifer transmissivities, aquitard resistances, drainage conductances, and the conductances of the groundwater-surface water exchange.

To evaluate the reliability of the model, NHI currently is extensively validated, in close collaboration with a broad group of stakeholders (Rijkswaterstaat, provinces, water boards and drinking water companies) covering the entire country, each bringing in their system knowledge and validation field data (Klopstra et al., 2021 in prep, Janssen et al., 2021 in prep). Recommendations for model improvement resulting from this validation will be implemented in the next version of the national model.

4.2 Regional groundwater model used in de pilot Raam

The regional NHI model of De Raam is developed by Waterboard Aa en Maas, based on the same software and data as in NHI-LHM 4.1. However, the spatial discretization is more refined and more detailed information is used. Therefore, the model is better equipped for regional analysis than the national model. The most important differences with the national model are:

- The grid size is 25x25 m (instead of 250 m);
- The subsurface is divided into 19 layers (instead of 8 layers);

- The meteorology is based on data from Meteobase (http://www.meteobase.nl), which includes extra radar data (instead of data from weather and precipitation stations of the Royal Dutch Meteorological Institute KNMI);
- The surface water levels in the smallest water bodies (the small ditches) are derived from a detailed Digital Elevation Model (DEM: the surface elevation along the ditch). This yields more detailed information for the surface water levels compared to the database of the waterboards used in the national model;
- The regional modules for the unsaturated zone (MetaSWAP) and for groundwater (MODFLOW) can be coupled to a hydraulic model for the surface water (instead of using only surface water routing through MOZART and the Distribution Model DM). Note that this has not been applied for the analysis of the TACTIC climate change in this report.

The groundwater model has been calibrated, based on measurements of groundwater heads in the period 2007 - 2016 (Bos-Burgering and Hunink, 2020).

4.3 Metran

The software Metran (Berendrecht & van Geer, 2016) is used for the time series modelling (Zaadnoordijk et al., 2019). The groundwater level time series is split into a deterministic part and a stochastic part (*Figure 4.2*). The deterministic part represents the variation due to the specified explanatory variables. For the models on the 'groundwatertools' website (http://www.grondwaterstandeninbeeld.nl), these are precipitation and potential evapotranspiration. It is possible to include additional influences, like surface water levels or a general trend. The difference between the deterministic part and the measurements is called the model residual.

A noise model is used for the stochastic part. The purpose is to remove the autocorrelation in the residuals. The smaller the time steps between the measurements, the larger the autocorrelation. The existence of autocorrelation decreases the reliability of the model. We use a noise model with an exponential decay. The inverse of the noise model is applied to the residuals to obtain so-called "innovations".

The explanatory variables are convoluted with an impulse response function (see e.g. Kreyszig, 2012): the value of each day is multiplied by the response function and the results are summed. An incomplete gamma distribution is used for the impulse response function (Berendrecht & Van Geer, 2016). It has three parameters, a multiplication factor A* and two shape parameters a and n (Besbes & de Marsily, 1984). For the groundwatertools website, the same function is used for precipitation and potential evapotranspiration except for a factor. This leads to five parameters to be optimized: three of the precipitation response, one evaporation factor, and one noise model parameter. The parameters are determined by a minimization procedure for the innovations.

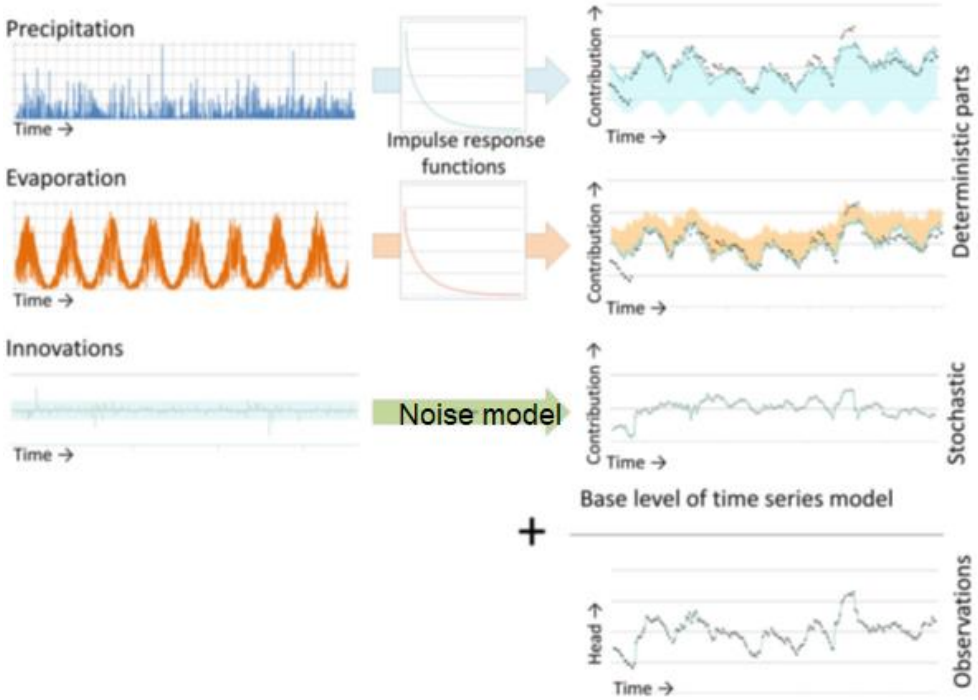

Figure 4.2 Setup of transfer function-noise model used for modelling head time series in Metran

The resulting time series models are evaluated using model evaluation criteria among which the explained fraction of the groundwater variation (Zaadnoordijk et al., 2019). Three classes are distinguished: bad models, reasonable models, and good models. The bad models are not shown on the website. The analysis in this report uses only the good models.

4.4 Climate change scenarios

In order to arrive at results that are inter-comparable for all of Europe a new procedure for selection of climate change scenarios has been developed within TACTIC.

The climate change scenarios have been based on climate data from the Inter-Sectoral Impact Model Inter-comparison Project (ISIMIP). These data consist of ensembles of 15 models: three Representative Concentration pathways (RCP) applied to five Global Climate Models. The spatial resolution is 0.5° and the temporal resolution 1 day. Two criteria were used to select an ensemble member (Sperna Weiland et al., 2021, in prep.):

- a global warming level of +3 degrees and +1 degrees, relative to a reference period (1980-2010);
- the 2nd highest and 2nd lowest scenario are selected, using the following indicators for regional climate change response: European mean temperature change, regional (case specific) precipitation change, regional net precipitation change and regional temperature change.

4.4.1 TACTIC standard Climate Change scenarios

The TACTIC standard scenarios are developed based on the ISIMIP (Inter Sectoral Impact Model Inter-comparison Project, see www.isimip.org) datasets. The resolution of the data is 0.5°x0.5° global grid and at daily time steps. As part of ISIMIP, much effort has been made to standardise the climate data (a.o. bias correction). Data selection and preparation included the following steps:

1. Fifteen combinations of RCPs and GCMs from the ISIMIP data set where selected. RCPs are the Representative Concentration Pathways determining the development in greenhouse gas concentrations, while GCMs are the Global Circulation Models used to simulate the future climate at the global scale. Three RCPs (RCP4.5, RCP6.0, RCP8.5) were combined with five GCMs (noresm1-m, miroc-esm-chem, ipsl-cm5a-lr, hadgem2-es, gfdl-esm2m).
2. A reference period was selected as 1981 – 2010 and an annual mean temperature was calculated for the reference period.
3. For each combination of RCP-GCM, 30-years moving average of the annual mean temperature where calculated and two time slices identified in which the global annual mean temperature had increased by +1 and +3 degree compared to the reference period, respectively. Hence, the selection of the future periods was made to honour a specific temperature increase instead of using a fixed time-slice. This means that the temperature changes are the same for all scenarios, while the period in which this occur varies between the scenarios.
4. To represent conditions of low/high precipitation, the RCP-GCM combinations with the second lowest and second highest precipitation were selected among the 15 combinations for the +1 and +3 degree scenario. This selection was made on a pilot-by-pilot basis to accommodate that the different scenarios have different impact in the various parts of Europe. The scenarios showing the lowest/highest precipitation were avoided, as these endmembers often reflects outliers.
5. Delta change values were calculated on a monthly basis for the four selected scenarios, based on the climate data from the reference period and the selected future period. The delta change values express the changes between the current and future climates, either as a relative factor (precipitation and evapotranspiration) or by an additive factor (temperature).
6. Delta change factors were applied to local climate data by which the local particularities are reflected also for future conditions.

Table 4-1 shows the RCP-GCM combinations employed for the analysis of the Dutch pilots in the TACTIC project. The average delta change factors for precipitation and evaporation for the national pilot and the pilot De Raam are shown in *Table 4-2* and *Table 4-3*, respectively.

Table 4-1. Combinations of RCPs-GCMs used to assess future climate

		RCP	GCM
1-degree	"Dry"	4.5	noresm1-m
	"Wet"	6.0	miroc-esm-chem
3-degree	"Dry"	6.0	hadgem2-es

	"Wet"	8.5	miroc-esm-chem

Table 4-2. Average delta change factors per climate change scenarios for the national pilot.

Netherlands	P	PET
1°C min	0.986	1.087
1°C max	1.056	1.086
3°C min	0.969	1.082
3°C max	1.139	1.087

Table 4-3. Average delta change factors per climate change scenarios for pilot De Raam

Pilot area: Raam	P	PET
1°C min	0.985	1.089
1°C max	1.051	1.093
3°C min	0.973	1.081
3°C max	1.146	1.094

The yearly averaged factors in *Table 4-2* and *Table 4-3* show only small differences for the national pilot and the regional pilot De Raam. The monthly factors show some more variation as can be seen in *Figure 4.3*. This illustrates the deviations that may be expected when applying a single set of change factors for an area as large as the Netherlands.

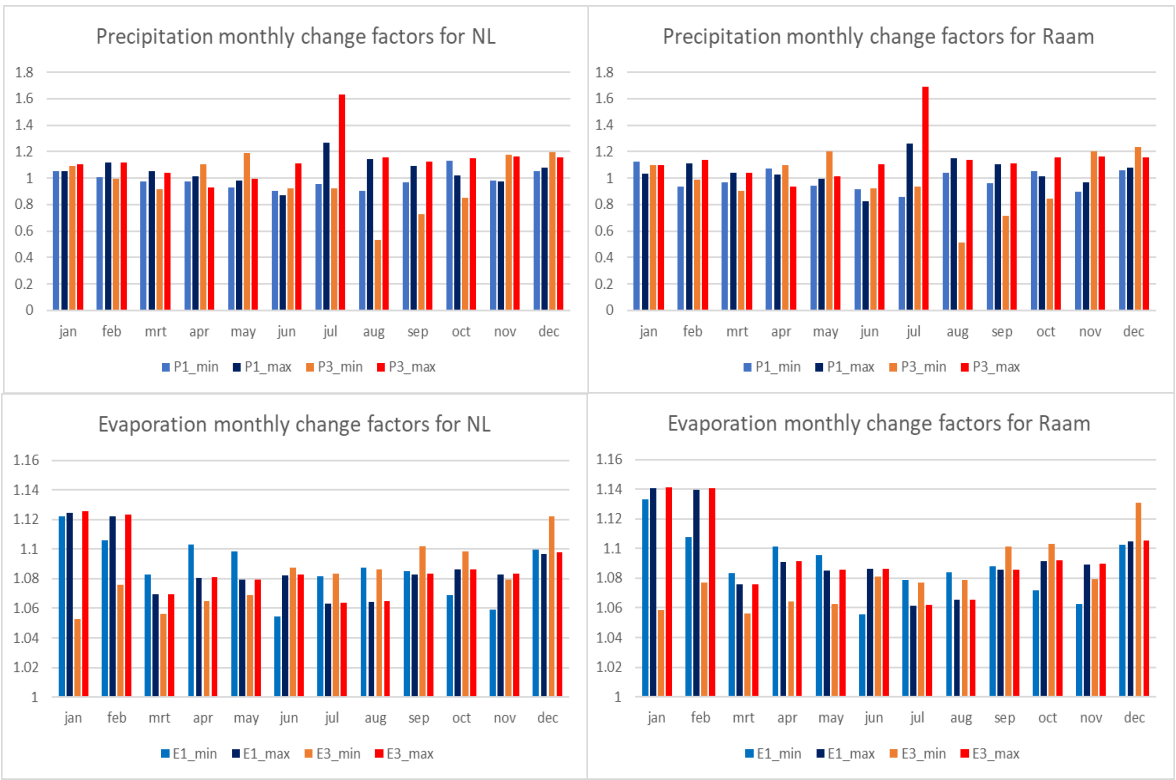

Figure 4.3. Delta change factors per month for the Netherlands (left) and De Raam (right).

5 RESULTS

This chapter presents the results for the national pilot and the pilot De Raam in separate sections (Section 5.1 and 5.2). Within these sections, results are presented for the reference period and the climate scenarios. Within these subsections the Integrated hydrological modelling (NHI) and the time series modelling are discussed independently.
Comparisons between the results in the various subsubsections are presented in the Discussion chapter (Chapter 6).

5.1 National pilot

The national pilot covers the entire country of Netherlands.

5.1.1 Reference period results

5.1.1.1 Integrated hydrological model

This subsubsection gives the results of the integrated model (NHI-LHM, see Section 4.1) of the national pilot. The model simulations have been carried out with LHM version 4.1. Although larger time series have been calculated with the model for the reference period, from 1980 - 2020, the following analysis focusses on the results in the period 2011 – 2018. This period is used more often for analyses of results of the national model, because extensive measurement sets are also available for this period, which allows extended validation of the model results. Besides, for this period also results are available for the regional pilot, which makes it easier to compare the national and regional approach.

In Figure 5.1, the phreatic head distribution and the deep groundwater heads are shown, averaged over the simulation period 2011 – 2018. The deep groundwater heads are the heads in Layer 4 of the model. Layer 4 is chosen, because this layer contains most of the groundwater abstraction wells in the Netherlands. In *Figure 5.2*, the typical winter and summer phreatic head are shown. The left picture is the typical winter head, which can be considered as the highest mean. This is a typical Dutch statistic of the water table depth. It is calculated as the yearly mean of the three highest phreatic heads calculated on every 14th and 28th day in a month, which is then averaged over the simulation period (in this analysis: 2011-2018). Similarly, the typical summer head (figure on the right), is calculated as the mean of the three lowest phreatic heads within a year, which is subsequently averaged over the same simulation period.

The average phreatic head illustrates the differences between the low-lying and higher parts of the Netherlands. In the reclaimed parts of the Netherlands (some typical polder areas mainly in the central and Western part of the Netherlands), the phreatic groundwater table is close to the ground surface. In the sandy ridges, the water table is at a higher depth below the surface area. A clear example is the Veluwe in the middle of the country, with phreatic heads at a depth of over 10 meter below ground level. In those typical infiltration areas with deep ground water levels, also higher model errors (> 1 m) might be found, when validation the model with measurements (figure 5.3). The typical winter and summer phreatic heads show the dynamics of the groundwater levels during a year. In the winter, the ground water level is almost at surface level in the Western and Northern parts of the Netherlands. In the driest period in the summer, the water table in these regions is about 1 meter lower compared to the winter situation.

Figure 5.1 shows that the deep groundwater heads in the regions with a low elevation are very high, often above surface level. This indicates that there is an upwards seepage flux in these areas.

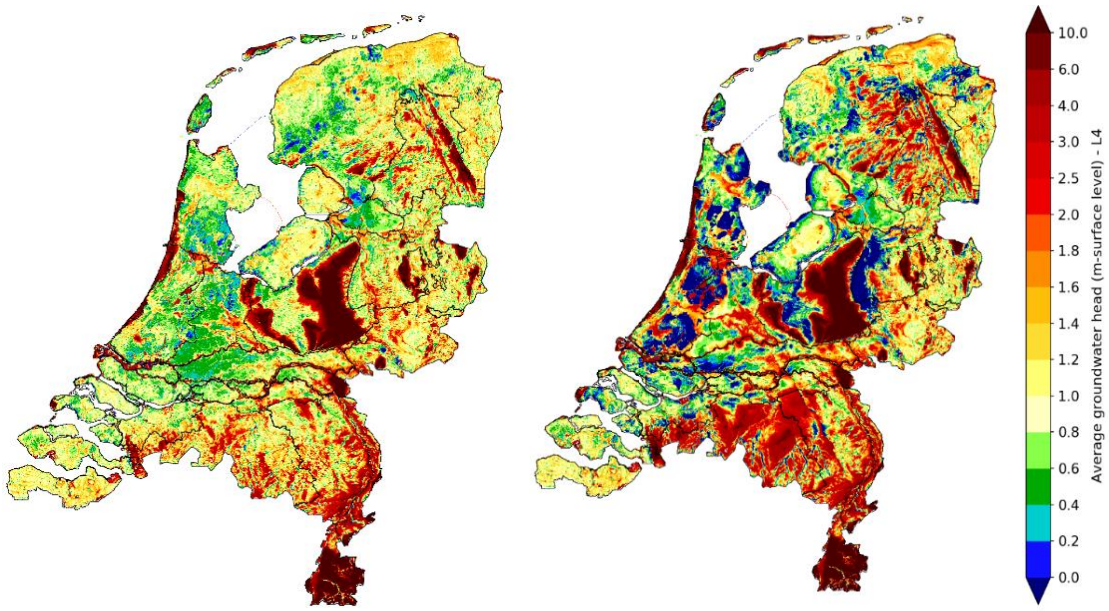

Figure 5.1. Average phreatic head (left) and deep groundwater head (model layer 4) in m below surface level.

Due to the seasonal variation mostly of evaporation and water use, the groundwater heads have a seasonal dynamic. This is illustrated by the high and low groundwater levels in *Figure 5.2*. These are the depth below the surface of approximately the 87.5th and 12.5th percentile of the groundwater table.

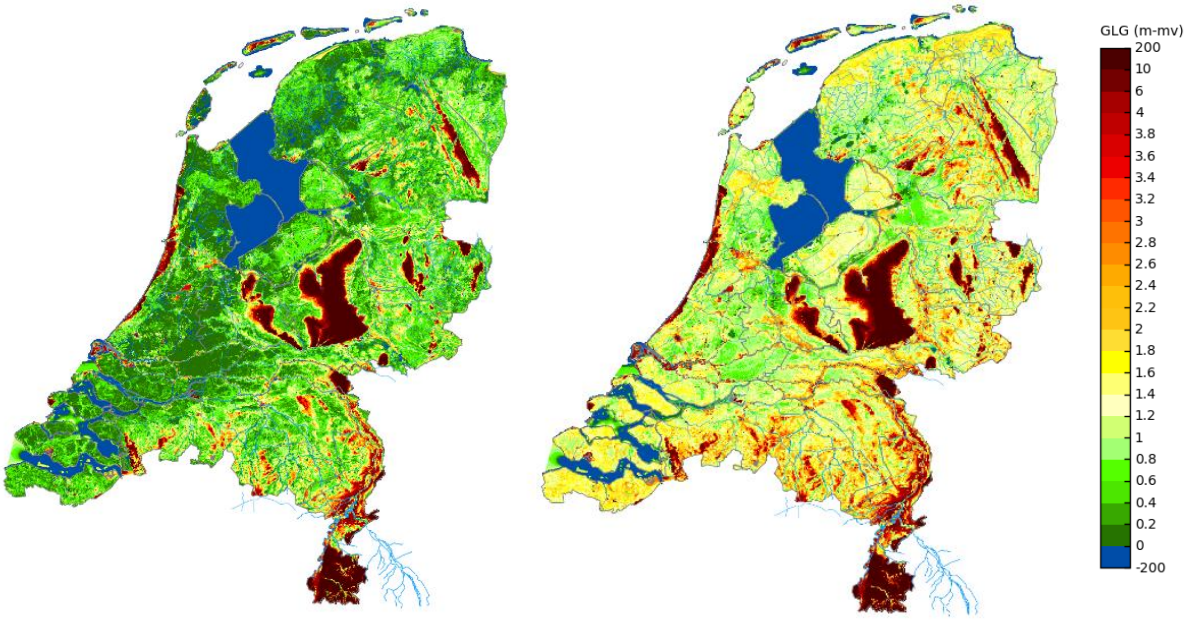

Figure 5.2. Average high (left) and low (right) groundwater levels in m below the surface level (approximately the 87.5th and 12.5th percentile).

The average high (GHG) and low (GLG) groundwater table is used for validation. *Figure 5.3* gives an example of the comparison of calculated and measured values for NHI-LHM version 4.1 for GHG, GLG and the difference between these (yearly dynamic).

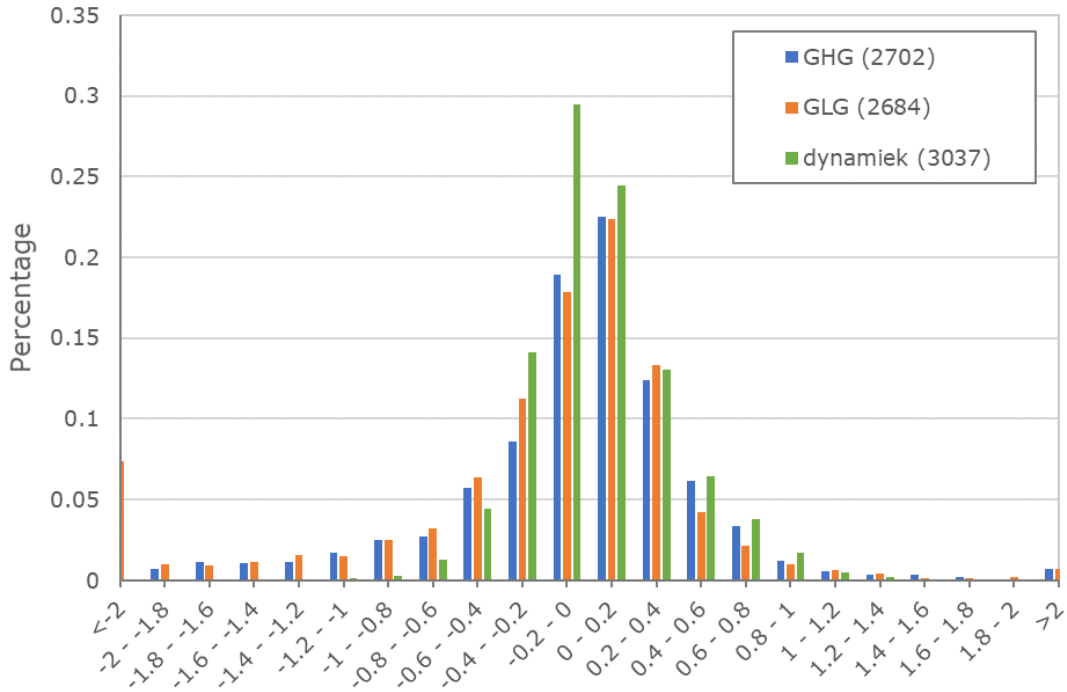

Figure 5.3. Example of validation of the calculated groundwater levels in LHM 4.1: the distribution (percentage on vertical axis) of prediction errors of calculated phreatic heads expressed in average high levels (GHG, approximately 87.5th percentile), average low (GLG, approximately 12.5th percentage), and the difference between GHG and GLG (yearly dynamics: "dynamiek"). Source: Berendrecht (2021).

NHI-LHM does not only calculate heads, but also fluxes. Due to the amount of detail in the schematization of the top system, groundwater recharge can be determined according to various definitions. *Figure 5.4* gives two examples: the effective precipitation and the recharge at the groundwater table.

The yearly effective precipitation is calculated as the difference between the yearly precipitation and the yearly potential evaporation. The left picture in *Figure 5.4* shows the average effective precipitation according to the national model (LHM) in the period 2011-2018. The reference situation shows that on a yearly basis, the Western and Northern part of the Netherlands are the areas that receive most precipitation. In these regions, the yearly average of the effective precipitation is positive. The South and East are dryer, where a small region stands out with negative effective precipitation (the higher potential evaporation is higher than the precipitation).

The groundwater recharge is calculated as the difference between the precipitation and the evapotranspiration and surface runoff, as calculated within the coupled models MetaSWAP and MODFLOW. This groundwater recharge which enters the upper boundary of the MODFLOW model is shown in the right picture of *Figure 5.4*. The reference situation shows that the calculated recharge is slightly higher in the lower part of the Netherlands: the Western and Northern areas. In the higher, sandy parts of the Netherlands, the recharge is slightly lower. These spatial differences are similar to the distribution of a high and low effective precipitation.

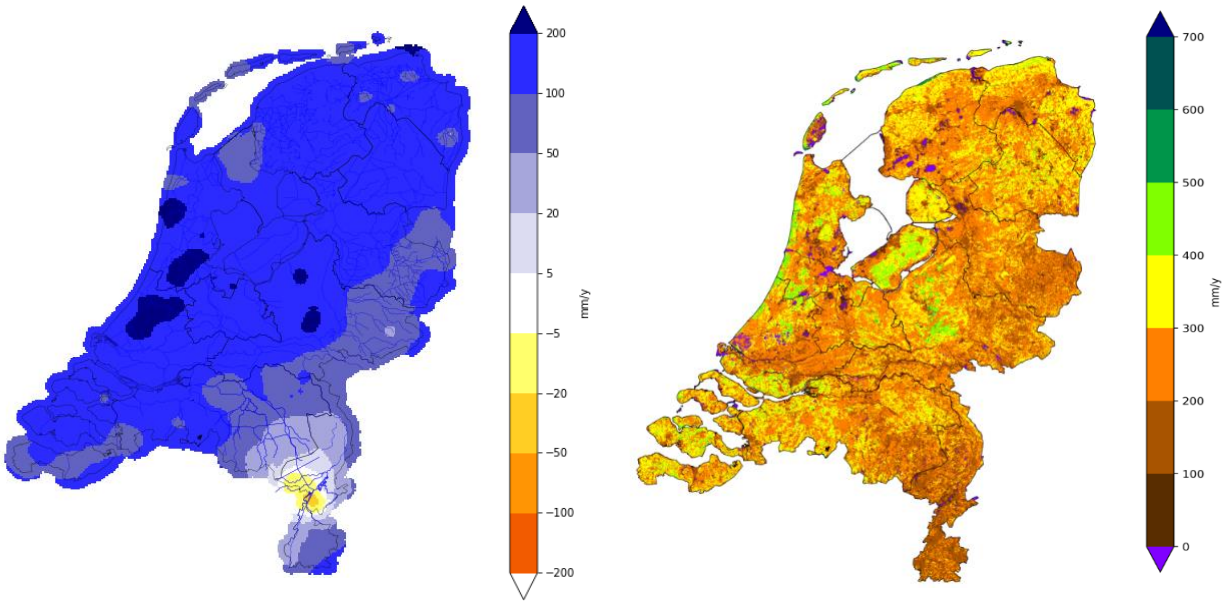

Figure 5.4. The average yearly effective precipitation in mm/year for the LHM (left) and average groundwater recharge in mm/year for the LHM (right)

Figure 5.4 illustrates that the recharge differs significantly from the net precipitation surplus, which mainly indicates large differences between reference evaporation (meteorological input for the model) and actual evapotranspiration (hydrological output of the model).

The surface water discharges, which are shown in *Figure 5.5*, contain the fluxes for all surface water systems as calculated by MODFLOW (DRN and RIV systems). The direction of these fluxes are relative to the groundwater system. This means that a negative flux describes water that is abstracted from the groundwater, whereas a positive flux is water that infiltrates the groundwater system. The discharge flux is generally negative, meaning the surface water bodies gain water from the groundwater. The West and North of the country have a very high density of surface water bodies, whereas the East and South show larger areas without surface water discharge.

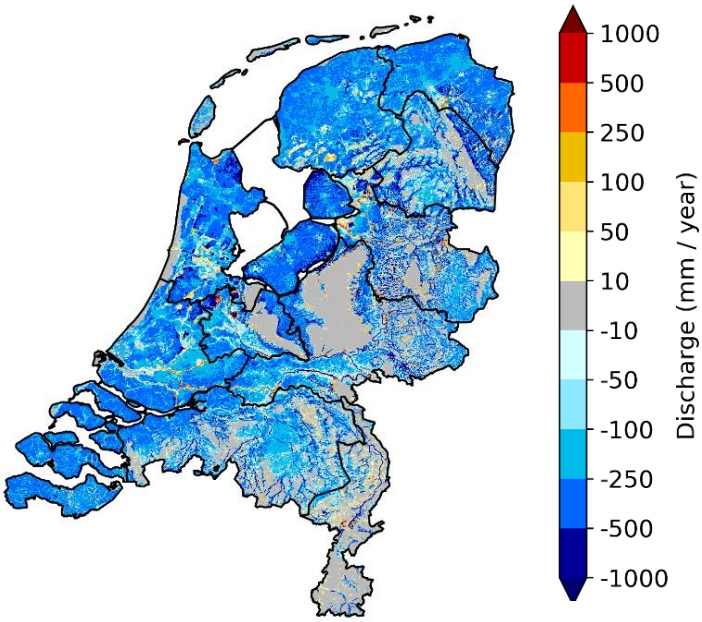

Figure 5.5. Average discharge of all surface water systems in mm/year

5.1.1.2 Time series models

The ground water tools website http://www.grondwaterstandeninbeeld.nl provides time series models for all groundwater head time series of the piezometers in the national database with subsurface data https://www.DINOloket.nl/en/subsurface-data. The time series models have been created by Metran (see Section 4.3). The precipitation response is related to the properties of the groundwater system (Zaadnoordijk & Lourens, 2019). The response can be characterized by the total response (or unit step response, i.e. the final value of the groundwater head change due to unit step change of the precipitation) and the median response time. These values usually are reliable for the models of good quality (Zaadnoordijk, 2018). See Section 4.3 and Zaadnoordijk et al., 2019 for the quality assessment of the time series models.

Figure 5.6 shows the total response from the piezometers in the upper regional aquifer of NHI-LHM with a good time series model.

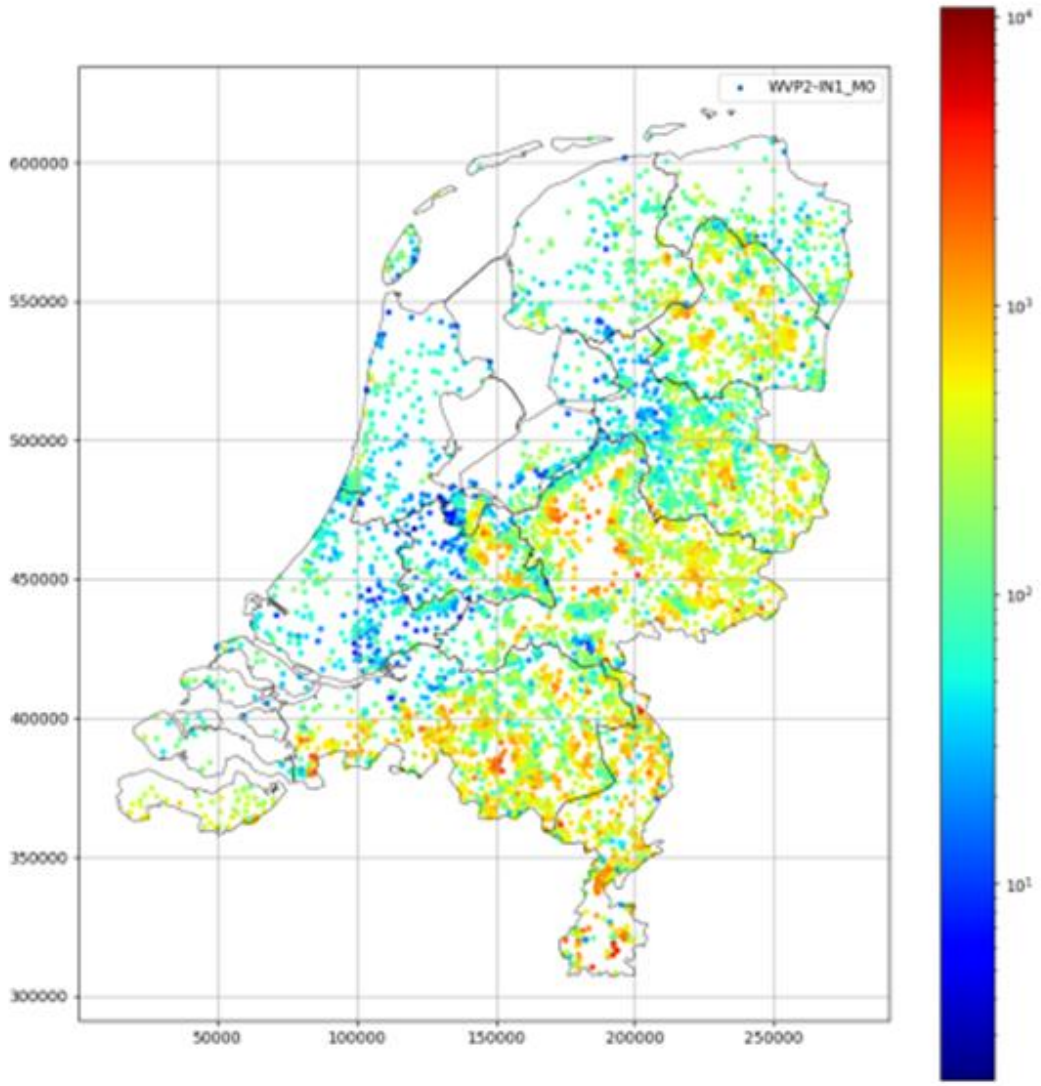

Figure 5.6 Total precipitation response (M0 or unit step response [100 day] groundwater head in cm over precipitation in meters per day) in the transfer-noise models for the upper regional aquifer (NHI-LHM code WVP2). Source: Zaadnoordijk & Lourens, 2019).

The pattern of the median precipitation response time in *Figure 5.7* is similar to that of the total response (*Figure 5.6*) with higher values in the East and South.

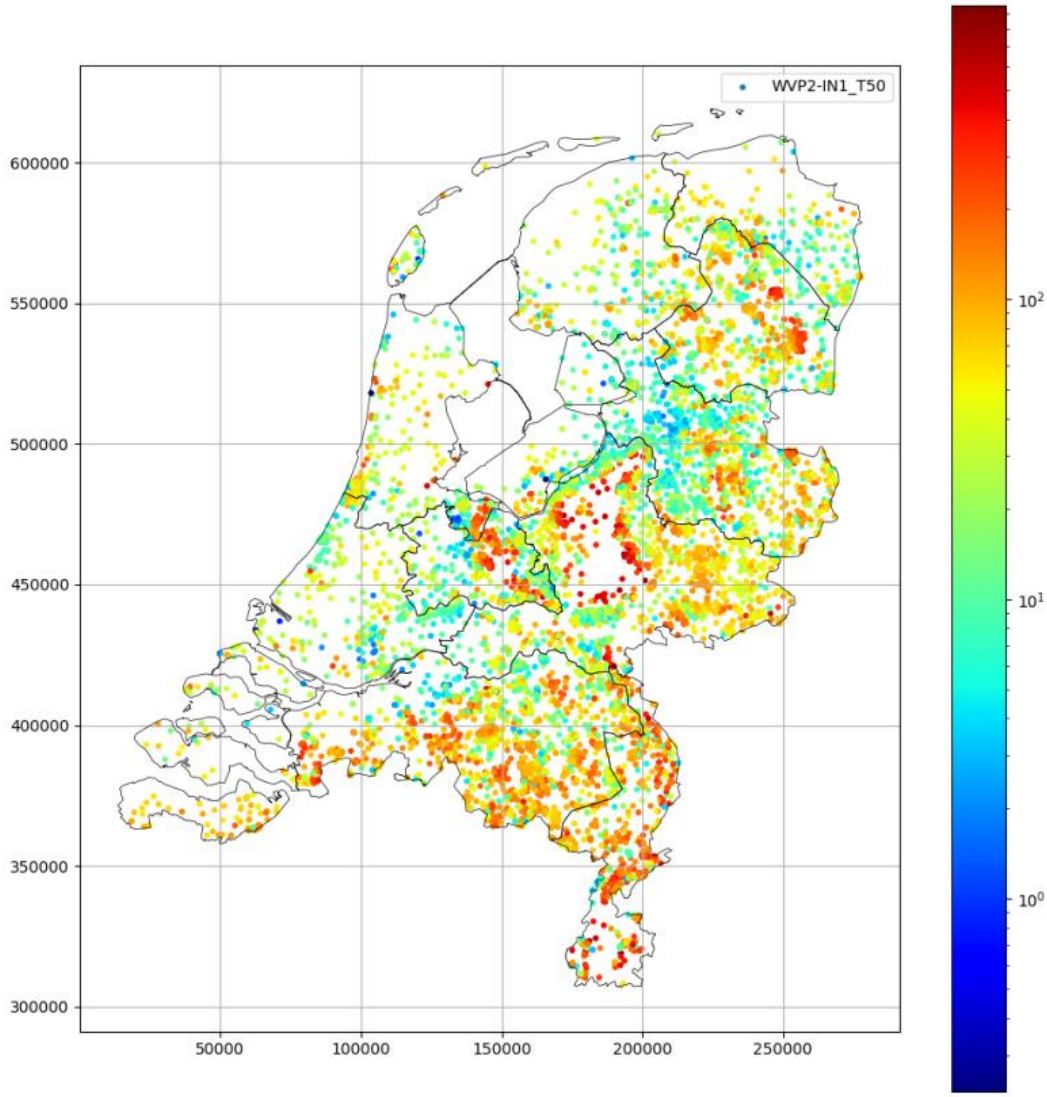

Figure 5.7 Precipitation response time (t50 [days]) in the transfer-noise models for the upper regional aquifer (NHI-LHM code: WVP2). Source: Zaadnoordijk & Lourens, 2019.

Under various assumptions, the evaporation coefficient of the Metran models can be used to determine a crude estimate of the long term average recharge (Obergfell et al., 2019). *Figure 5.8* and *Figure 5.9* show the values on a map for the piezometers located in the two upper model aquifers of NHI-LHM. The maps do not show an apparent spatial pattern. Comparisons of the Metran estimates with the groundwater recharge calculated by NHI-LHM are given in Sub-subsection 6.4.2.1 .

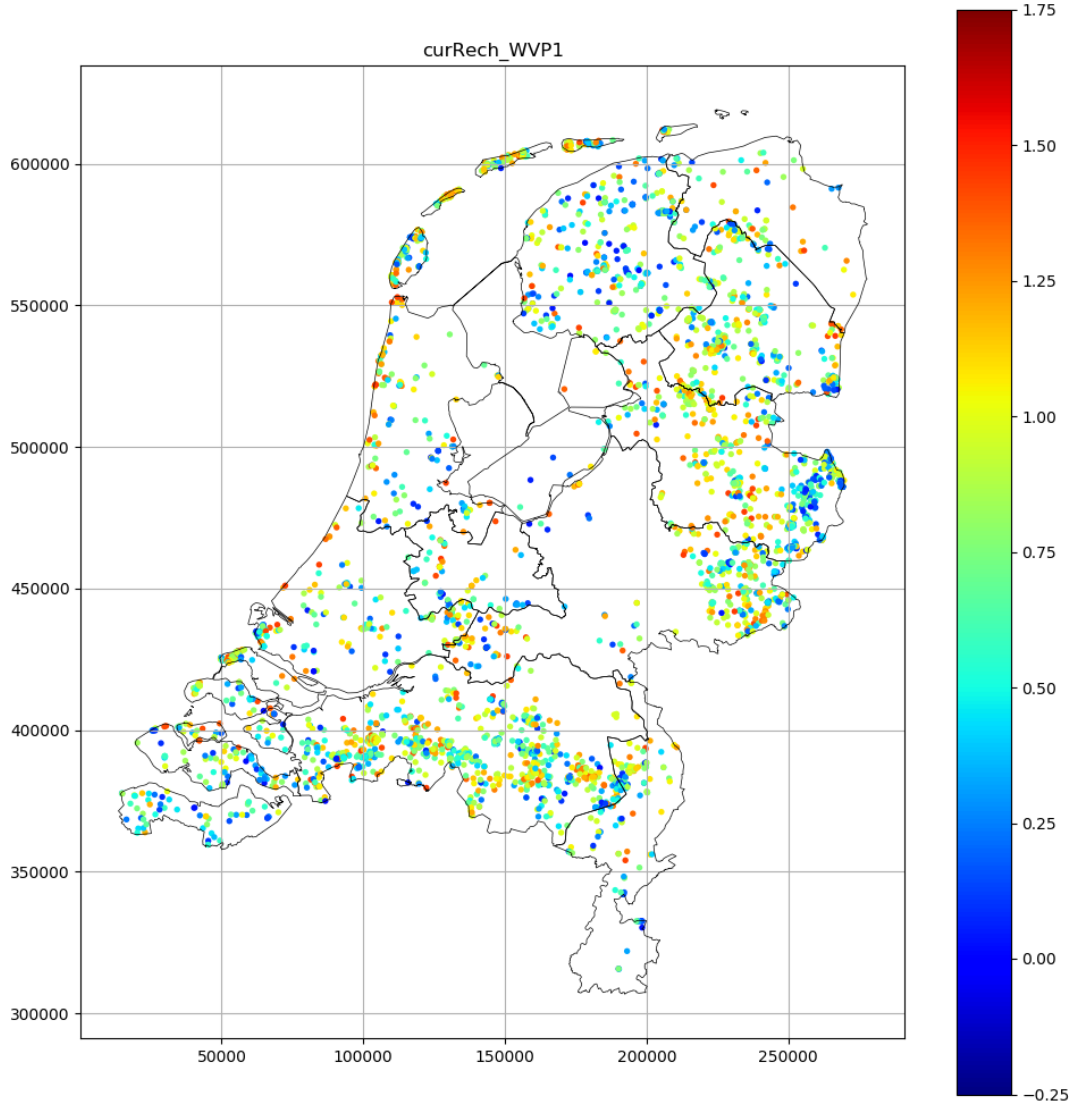

Figure 5.8 Crude estimate of groundwater recharge [mm/day] from evaporation factor in Metran models of piezometers in NHI-LHM modelaquifer 1 (phreatic water table aquifer).

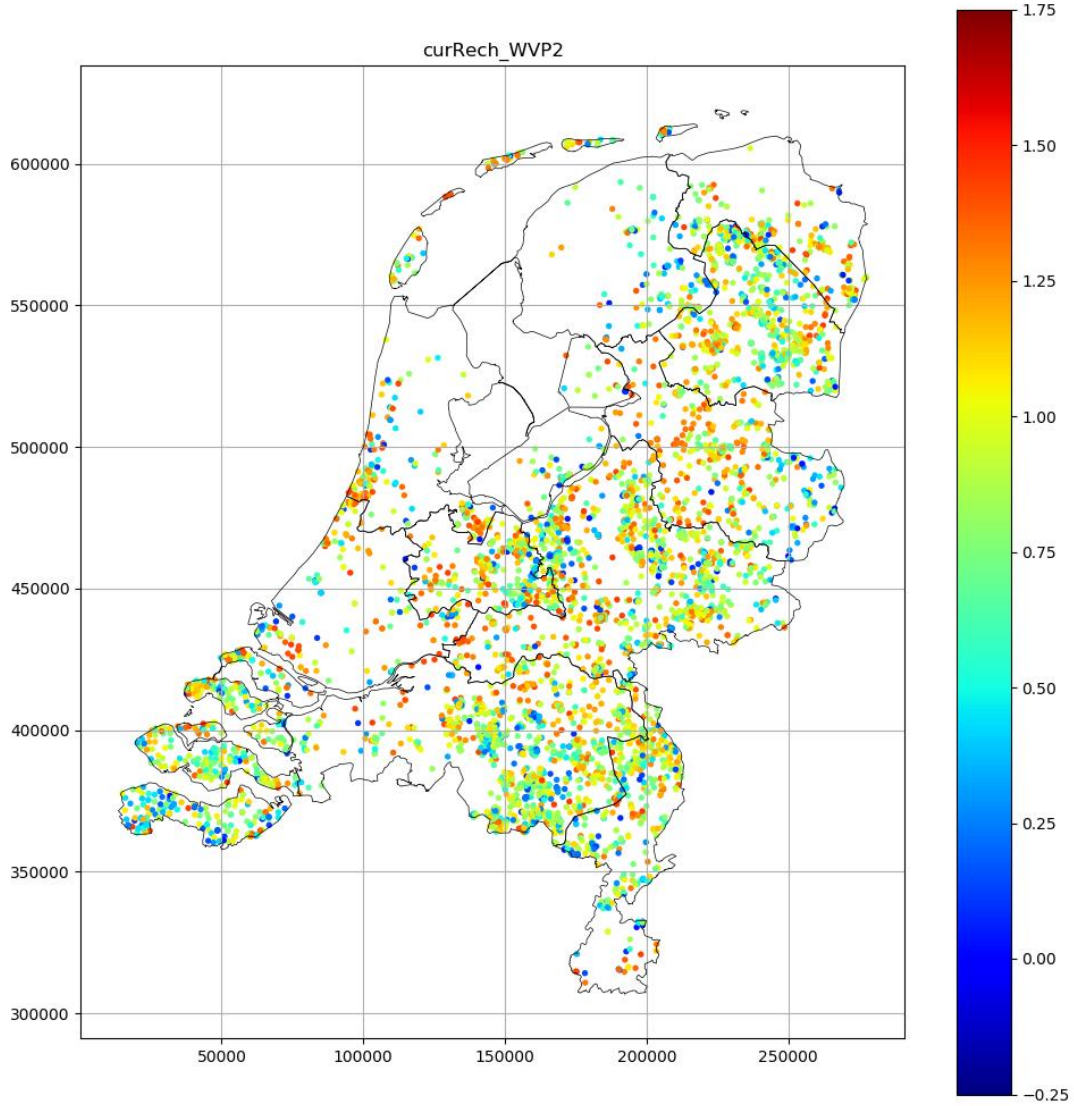

Figure 5.9 Crude estimate of groundwater recharge [mm/day] from evaporation factor in Metran models of piezometers in NHI-LHM modelaquifer 2 (the upper regional aquifer)

5.1.2 Climate change scenario results

This subsection contains results for the climate change scenarios described in section 4.4.

5.1.2.1 Integrated hydrological model

The effective precipitation in the reference situation and under the different climate scenarios is shown in *Figure 5.10*. The climate scenarios have a different impact on the effective precipitation. The regional differences that are visible in the reference situation remain the

same: the North and West have a higher effective precipitation compared to the South and East of the Netherlands. The 'dry' scenarios of both temperature rise scenarios (1° min and 3° min) reduce the effective precipitation. In the 3° min scenario, almost the whole South-eastern half of the country will have on average a negative effective precipitation. The 'wet' scenarios (1° max and 3° max) increase the effective precipitation. The national variation of the effective precipitation in the 1° max scenario is comparable to the reference situation, but the whole country has a positive effective precipitation. In the 3° max scenario, the effective precipitation is over 200 mm/year for a large part of the country. The differences between the minimum and maximum variants of the climate scenarios are mainly caused by a strongly varying precipitation flux for the different variants.

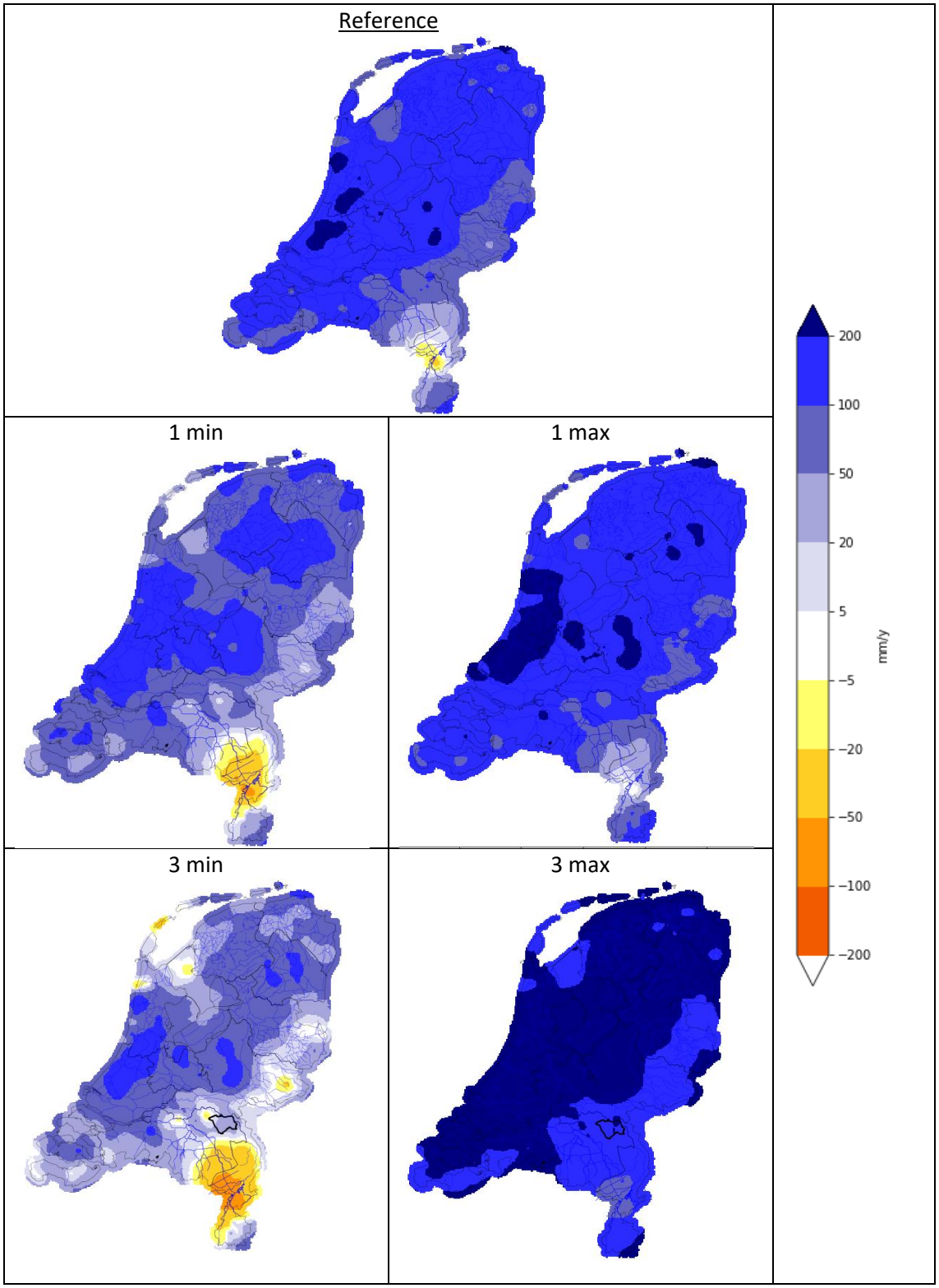

Figure 5.10. Average yearly effective precipitation (mm/year) for the reference situation (top) and the effect of the different climate scenarios (middle and bottom)

Figure 5.11 illustrates the effect of the climate scenarios on the phreatic groundwater head and *Figure 5.12* shows deeper groundwater heads. Generally, the 'dry' variants of the climate scenarios result in a decrease in the groundwater head, which means that the water table level decreases. On the contrary, the 'wet' scenarios result in an increase of the groundwater head and therefore increases the level of the water table.

The differences in heads due to climate change are larger in the South and East of the country compared to the low-lying areas in the North and West. The hydraulic head in these low-lying areas is generally very little affected in the 1° min scenario. In this scenario, only the regions with high surface elevations (the Veluwe and the South-eastern corner of the country) experience a decrease in phreatic head of about 0.5 – 1.0 m. For the 'dry' variant of 3 degrees temperature increase (3° min), the phreatic head is influenced in almost the whole country. This means that the phreatic head is lowered with at least 5 cm and locally up to 2 meters. The locations with the largest decrease in head in the 3° min scenario, are also the locations with the largest increase in phreatic head in the 3° max scenario. These sandy locations (the Veluwe for example) function as typical infiltration areas, where (change in) effective recharge directly leads to change in heights because the absence of surface waters. The increment in the phreatic head may locally exceed 2 m. In contrary, in the West of the Netherlands the changes are damped by the abundancy of surface waters.

The 3° max scenario hardly leads to changes in ground water heads, because the surplus of water is easily drained by the intensive drainage systems. The lower net precipitation in the 3° min scenario does have effect the ground water heads in the Western part of the Netherlands, because the lower net precipitation can't sufficiently be compensated by a surface water supply, while this can still be compensated in the 1° min scenario. This stresses the importance to have combined calculations for groundwater and availability of surface water for the Netherlands.

The 1° max scenario stands out from the other scenarios in the sense that there are regions that show an increase in head, as well as regions with a decreasing hydraulic head. The areas react differently in this scenario due to a difference in net precipitation, land use and geohydrological properties.

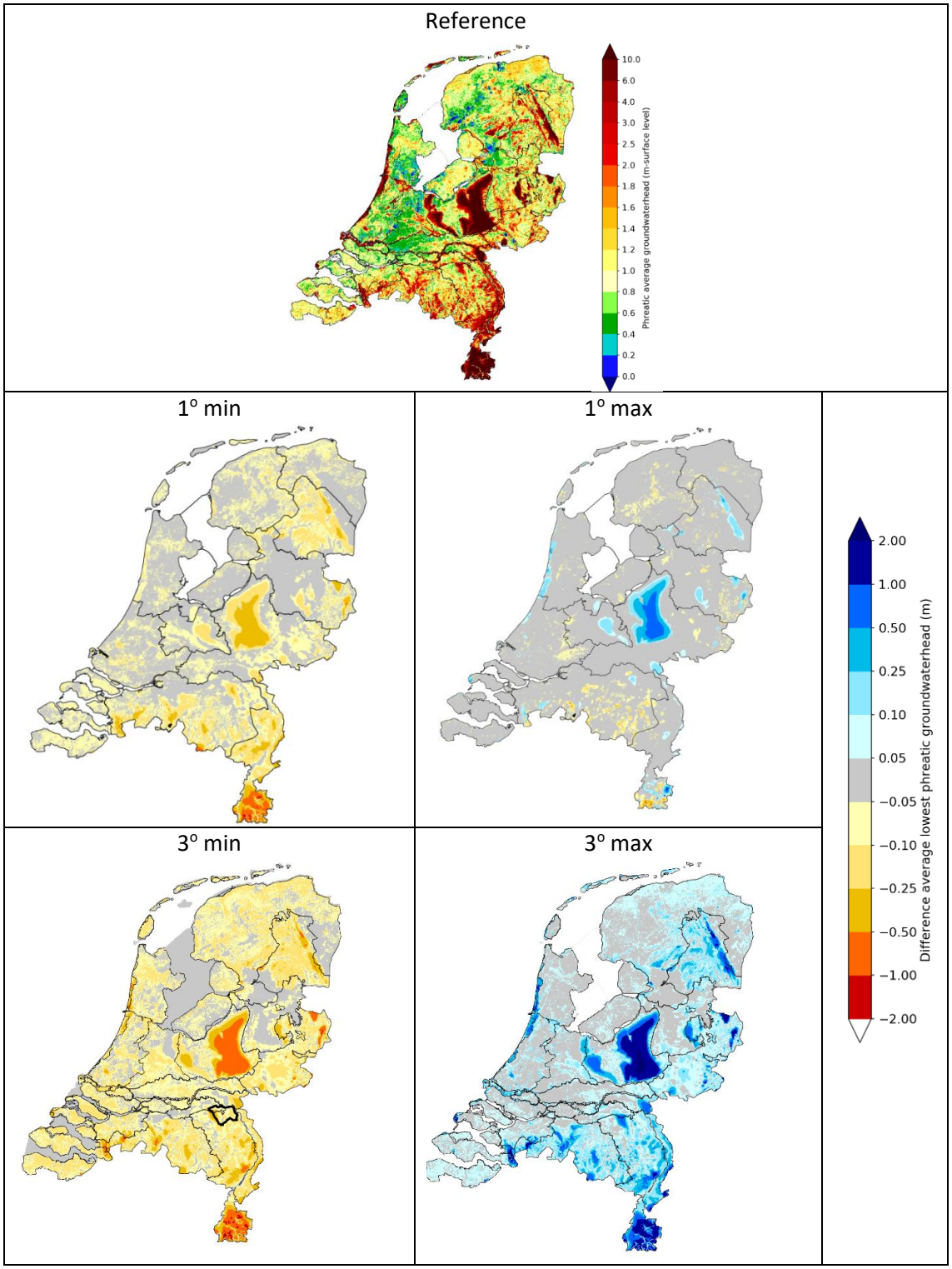

Figure 5.11. Average mean phreatic groundwater head in m below surface level (top) and the differences in mean phreatic groundwater head for all climate scenarios compared to the reference situation

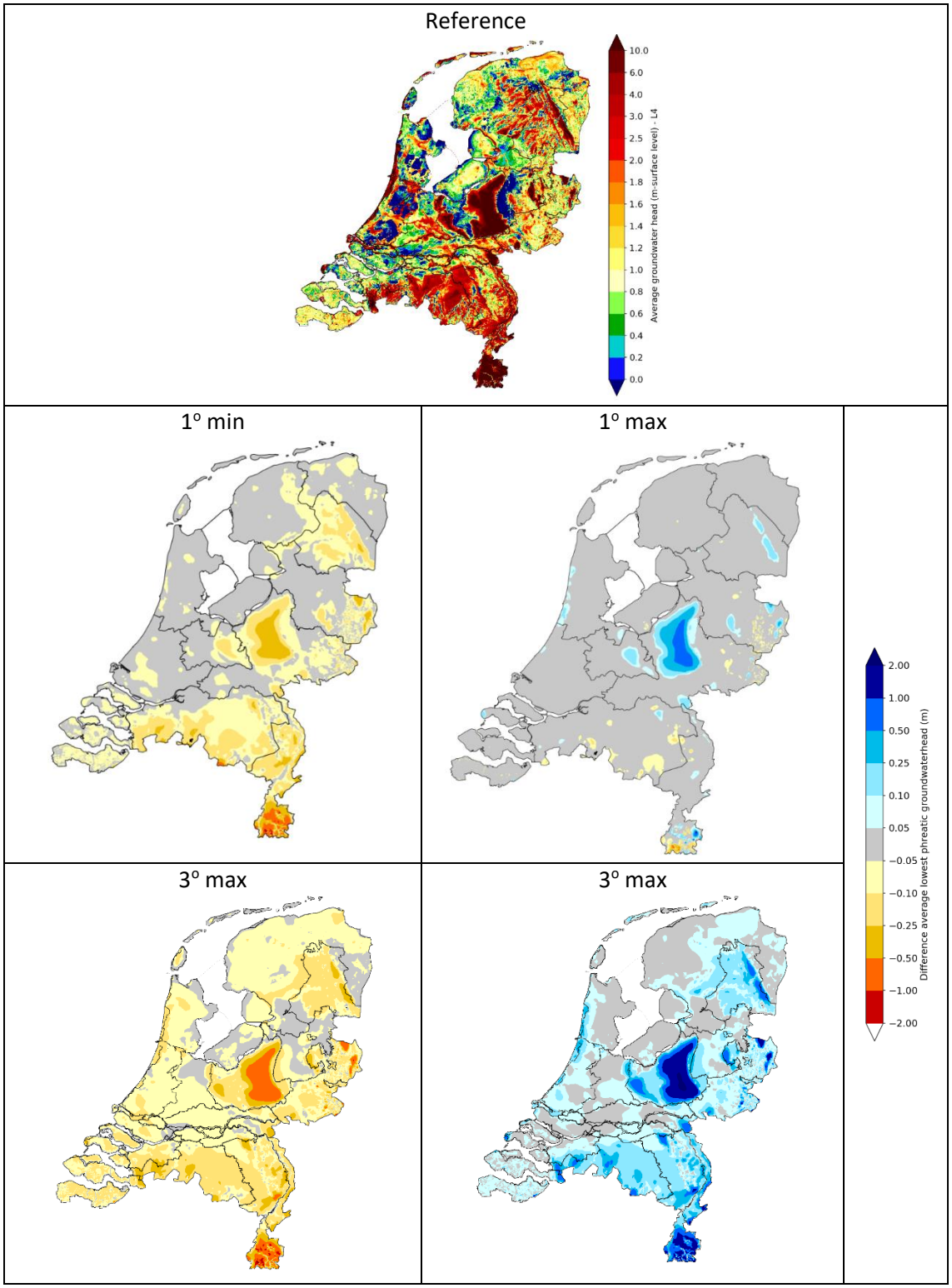

Figure 5.12. Average mean deep groundwater head (model layer 4) in m below surface level (top) and the differences in mean deep groundwater head for all climate scenarios compared to the reference situation.

The average groundwater recharge for the climate scenarios is shown in *Figure 5.13*. In the 1° min scenario, the recharge slightly decreases, mainly in the North-eastern part of the country. The 1° max scenario shows both an increase as a decrease in recharge, which is similar to the effect as shown for the heads. The regions where the hydraulic head increases, are also the regions with an increasing groundwater recharge. The 3° min scenario shows a decrease in recharge in almost the whole country, although this decrease is almost negligible in the very South. The 'wet' scenario (3° max) illustrates an increase in groundwater recharge, which is highest in the Northeast.

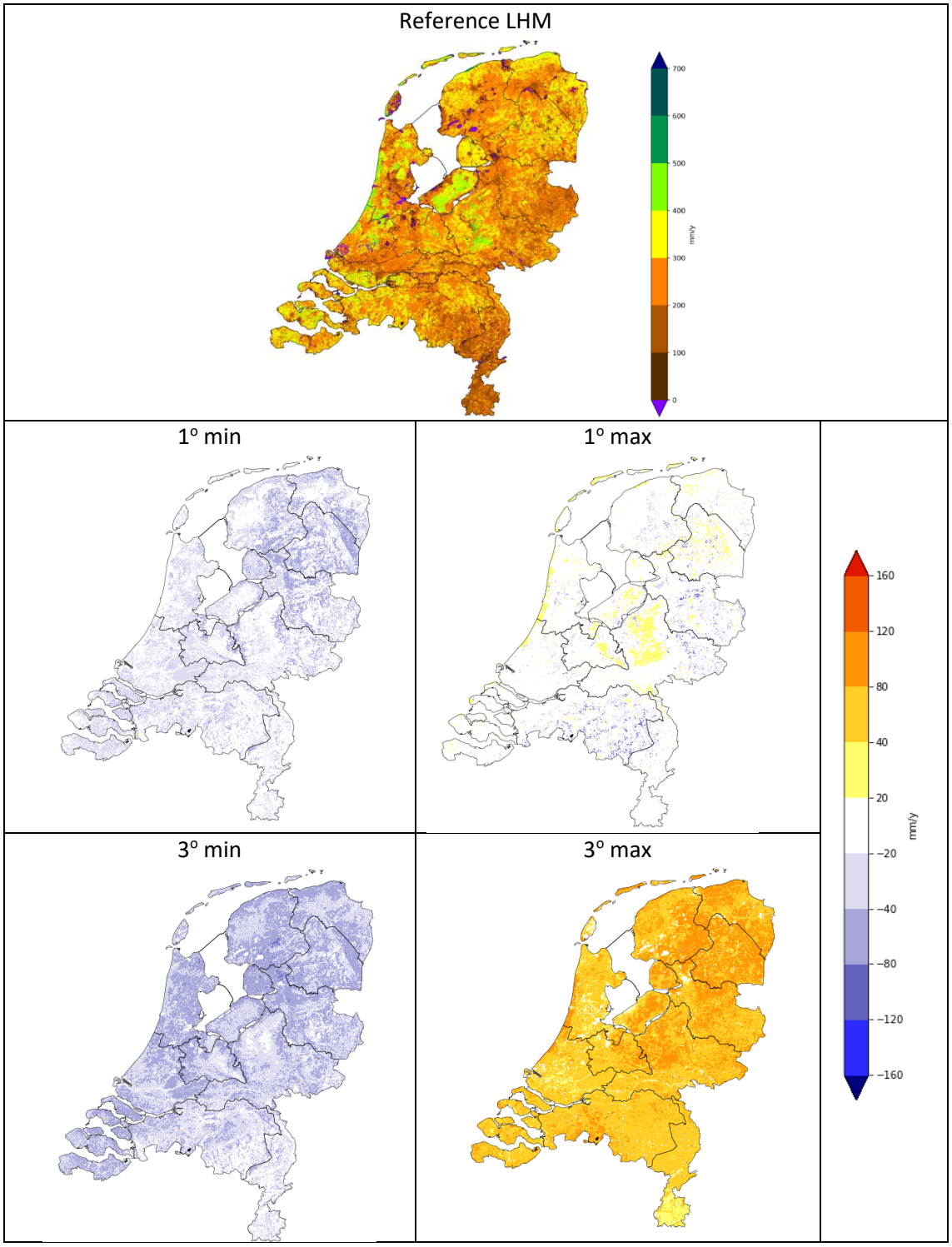

Figure 5.13. Average groundwater recharge in mm/year in 2011-2018. Top: groundwater recharge (mm/year) in the reference situation. Middle and bottom: difference in average groundwater recharge (mm/year) for the different climate scenarios compared to the reference situation.

In *Figure 5.14* the average nationwide recharge is plotted. The top left picture shows the average for every month in the whole simulation period, and compares the climate scenarios. Clearly, the biggest differences occur in the summer period (April – September). The 1° min and 3° min scenario have a lower recharge every month except for November and December, when the 3° min recharge exceeds the reference recharge. The 3° max scenario is clearly the wettest scenario, with a positive value in all months except April, May and June. The 1° max scenario shows an interesting pattern: it has the highest negative recharge in April, May and June, but abruptly switches to a slightly positive value in July.

The other graphs in *Figure 5.14* show the differences in recharge over the different years. To derive these graphs, the average recharge per month is calculated for every simulation year between 2011 and 2018. The lowest and highest value that is found for every month is shown as respectively the minimum and maximum value in *Figure 5.14*. These graphs show that the variation in recharge between years can be substantial. For example, the recharge in August was almost -0.5 mm/day in 2003, but more than +0.5 mm/day in 2004. In general, the 'dry' climate scenarios (1° min & 3° min) decrease this variability between years, whereas the 'wet' climate scenarios show an increased variability. To compare: the difference in the minimum average and maximum average recharge in August is in the reference situation about 1 mm/d, in the 3° min scenario about 0.5 mm/d and in the 3° max scenario about 1.25 mm/d.

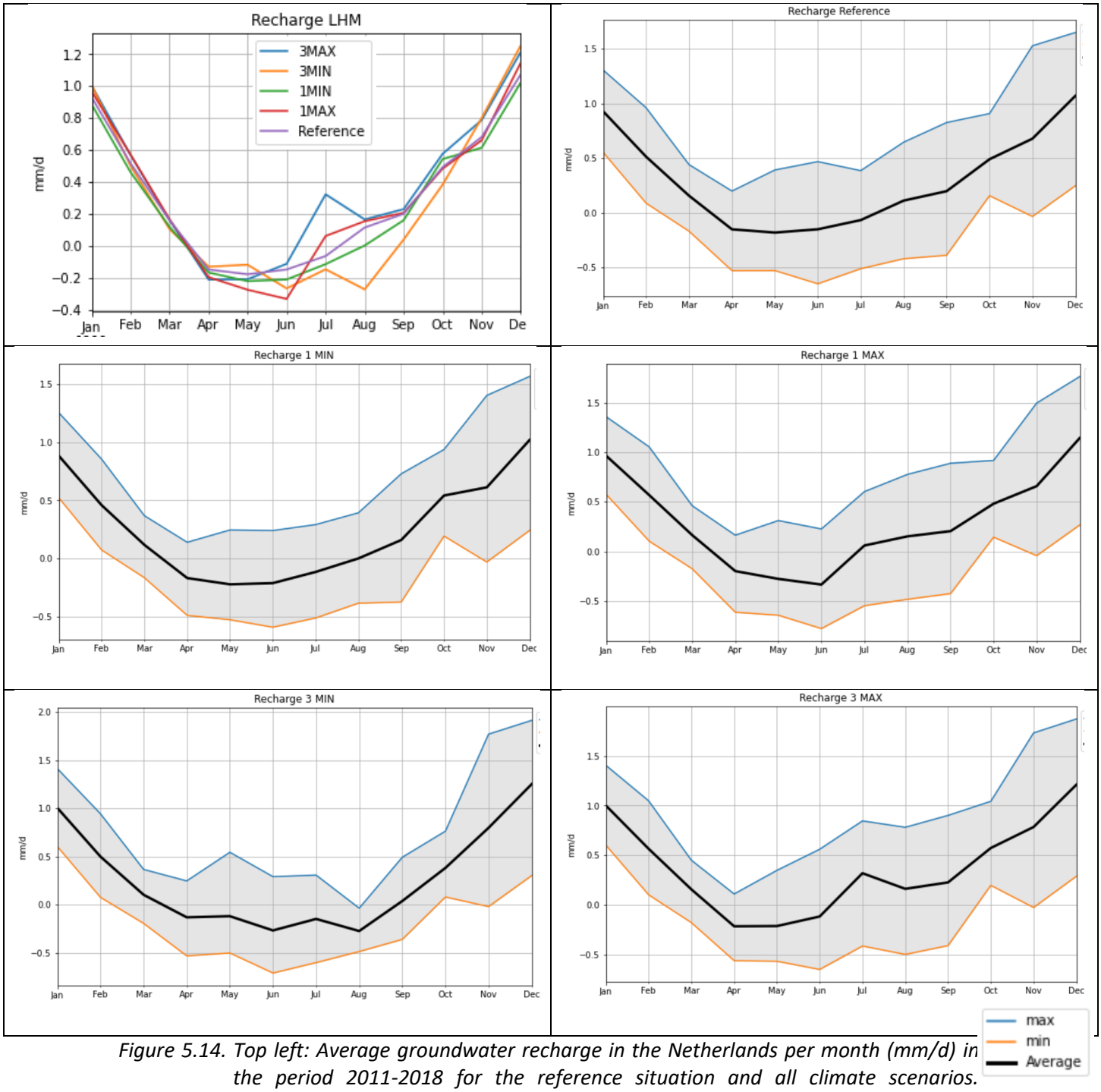

Figure 5.14. Top left: Average groundwater recharge in the Netherlands per month (mm/d) in the period 2011-2018 for the reference situation and all climate scenarios. Top right, middle and bottom row: average groundwater recharge per month and the maximum and minimum average groundwater recharge per month in the reference situation (top right) and the climate scenarios (middle and bottom row).

The effect of climate change on the discharges is relatively minor for the scenarios based on one degree temperature change, but may be significant for 3 degree temperature change (see *Figure 5.15*). In the latter case, differences in discharge reach up to 50 mm/year in many areas due to climate change, which is significant compared the total discharge of about 250 – 500 mm/year. The dry climate variants (the min scenarios) show a positive increase in the discharge flux. This means that the flux becomes less negative and the total discharge decreases. In the 1 degrees scenario, only the discharges in a limited amount of water bodies are affected; in the Western part of the Netherlands the effect is limited by the damping effect of the surface water systems. In the 3° min scenario, all surface water bodies are affected.

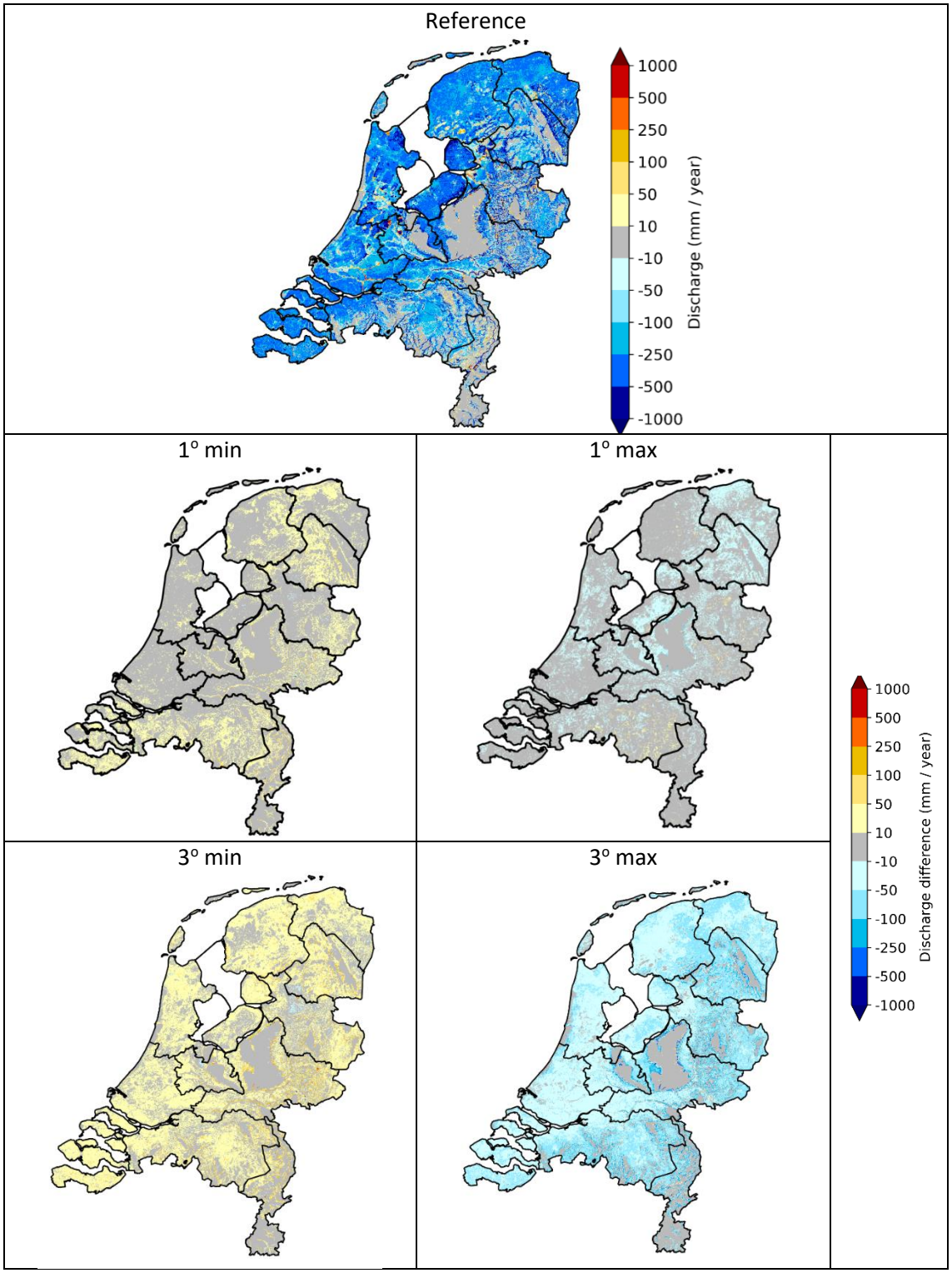

Figure 5.15. Average discharge of all surface water systems in mm/year in the reference situation (top) and the differences in discharge for all climate scenarios compared to the reference situation

5.1.2.2 Time series models

The piezometers selected for the regional pilot (subsection 5.2.1.2) have been simulated with the national climate change factors (in addition to the regional factors – see subparagraph 5.2.2.2) and compared to the results of the national integrated model NHI-LHM. The results are inter-compared in section 6.3.

Furthermore, long term average recharges have been calculated for the climate scenarios. The results offer only an indication of the change, with little spatial variation, due to the crude calculating and the usage of uniform meteorological data for the entire country (*Figure 5.16*).

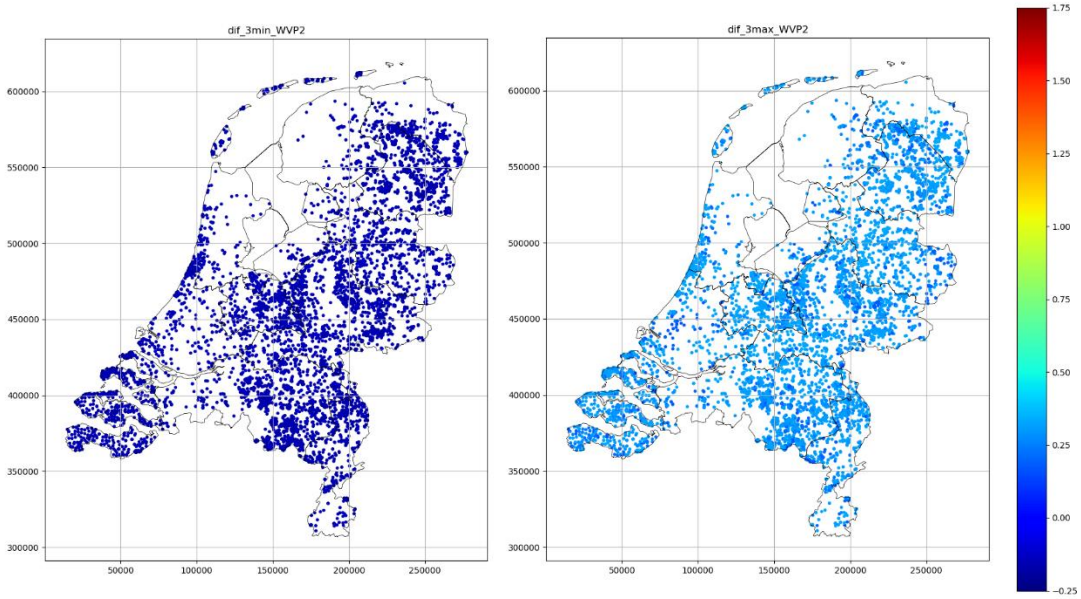

Figure 5.16 Change of the crude estimate of groundwater recharge from Metran models of piezometers in NHI-LHM model aquifer 2 for climate change scenario 3° min (left) and 3° max (right).

5.2 De Raam

5.2.1 Reference period results

5.2.1.1 Integrated hydrological model

The phreatic head distribution in pilot area 'De Raam' is shown in *Figure 5.17*. The Western part of the area has phreatic heads that a relatively far below the surface level. This is due to the fact that the surface elevation sharply increases towards this region: the elevation difference is about 8 m. Furthermore, the phreatic heads near the river Meuse are also relatively deep (far below surface level).

The groundwater recharge is shown in *Figure 5.18*. This picture shows that the groundwater recharge is quite uniform across the whole area. In the areas with land use type 'urban area' and 'forest' have the lowest groundwater recharges.

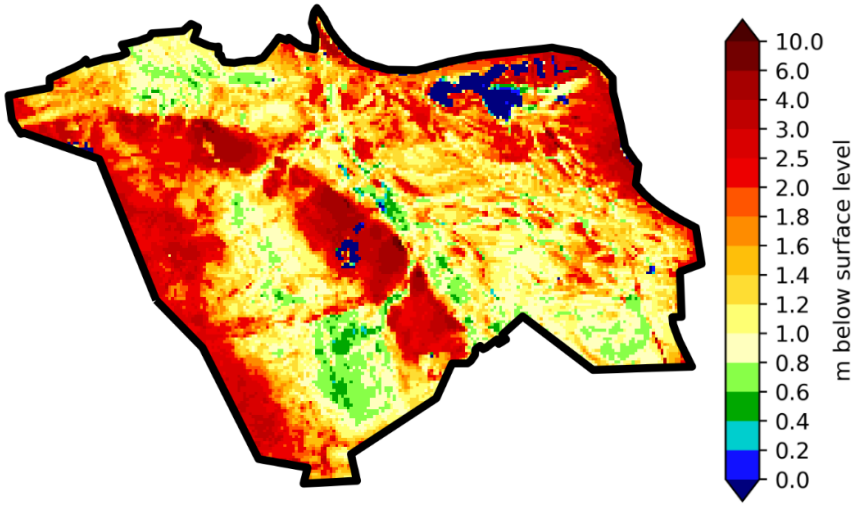

Figure 5.17. Average phreatic head in pilot area 'De Raam' in m below surface level.

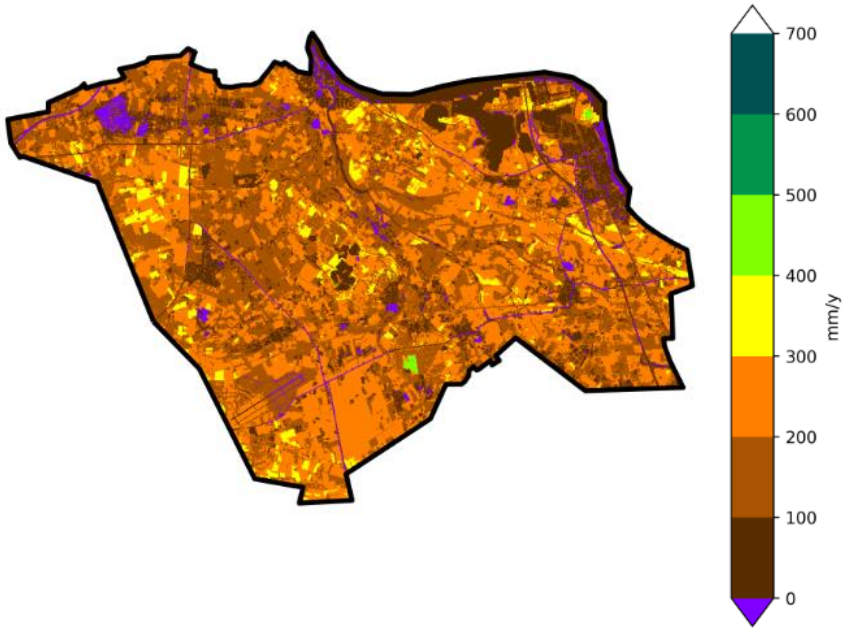

Figure 5.18. Average groundwater recharge in pilot area De Raam (mm/year) in period 2011-2018

5.2.1.2 Time series models

Metran (see section 4.3) has been used to create time series models for selected time series using precipitation and evaporation as explanatory variables to determine the precipitation response and to perform simulations for the climate scenarios (see subsubsection 5.2.2.2).

Also some time series along the river Meuse have been modelled with the river water level as a third explanatory variable in order to investigate the linearity of the river response under different circumstances.

Three monitoring wells have been selected to create time series models (see *Figure 5.19*). The wells have multiple piezometers at various depths.

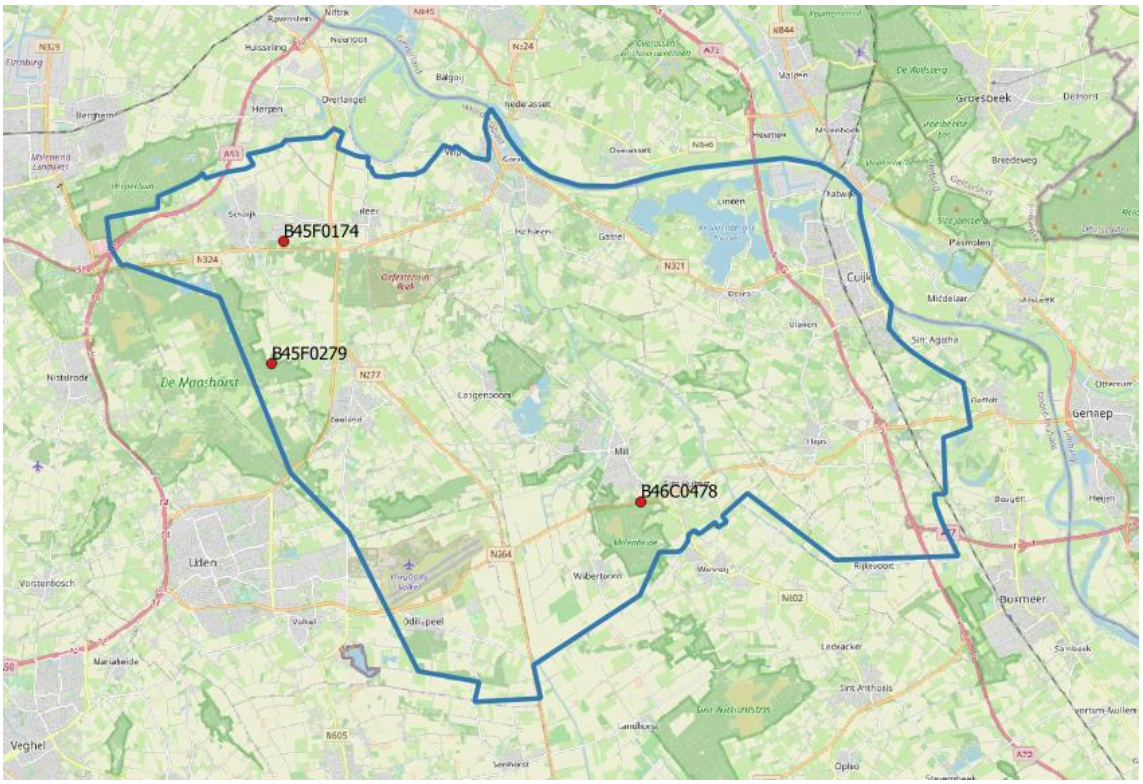

Figure 5.19 selected multi-piezometer monitoring wells for pilot de Raam.

Figure 5.20 and *Figure 5.21* show the median precipitation response time and the total precipitation response from the Metran models, respectively. The results show that these characteristics of the precipitation response are quite similar for all piezometers. They vary more in lateral direction compared to the vertical direction. This is due to the lack of aquitards with a high resistance and differences in conditions at the locations of piezometers.

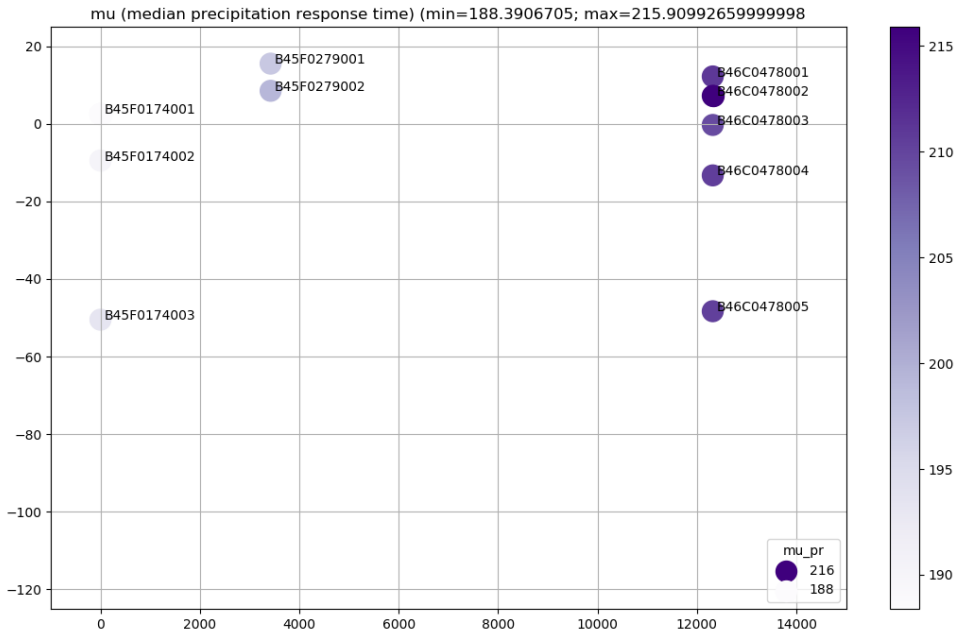

Figure 5.20 median precipitation response time [days] from Metran models of groundwater head time series with vertical coordinates in meters.

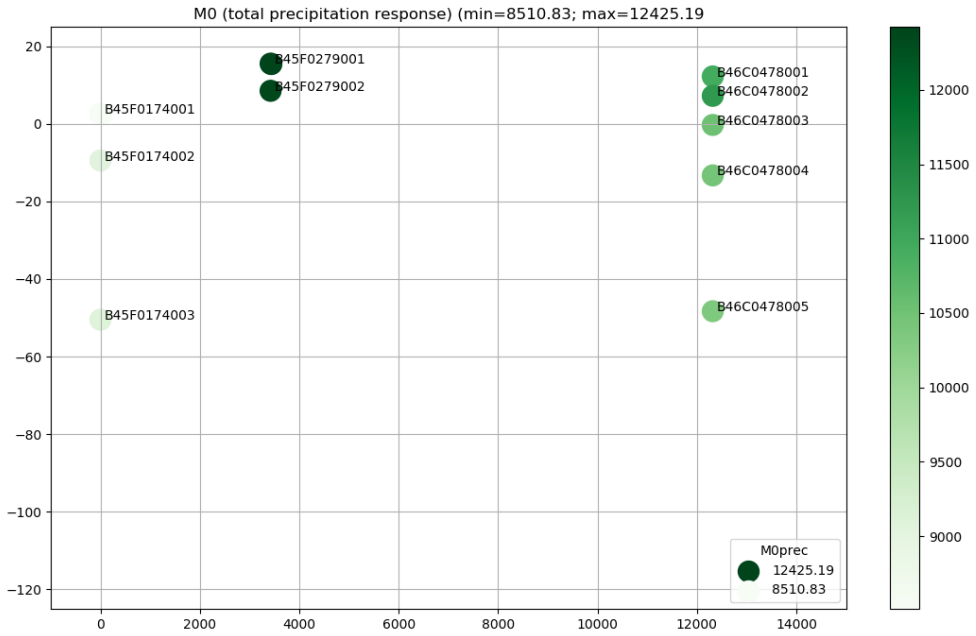

Figure 5.21 Total precipitation response [0.1 d] = [mm/(cm/d)] from Metran models of groundwater head time series with vertical coordinates in meters.

Time series modelling of groundwater response to river water levels

A shipping accident on the river Meuse in December 2016 offered an opportunity to look at the performance of Metran under unusual consequences. A ship rammed the weir in the river Meuse at the Western boundary of the pilot area of de Raam (downstream). This caused a drop of the Meuse water level of 3 meters (*Figure 5.22*), while the normal fluctuation is much smaller (and mostly upward during high discharge events).

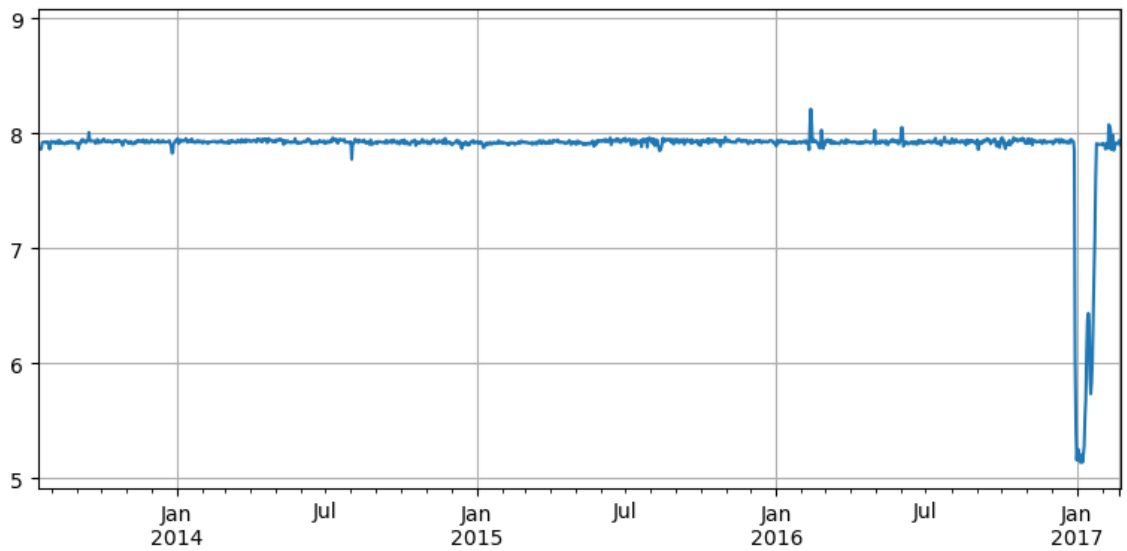

Figure 5.22 Meuse river level in meters above NAP

The groundwater in piezometer B46A1559001 at 160 meters from the Meuse reacts very quickly to the river level. Metran can match the slower response to precipitation and evaporation much better, but the timing and direction of the river response can be represented (*Figure 5.23*).

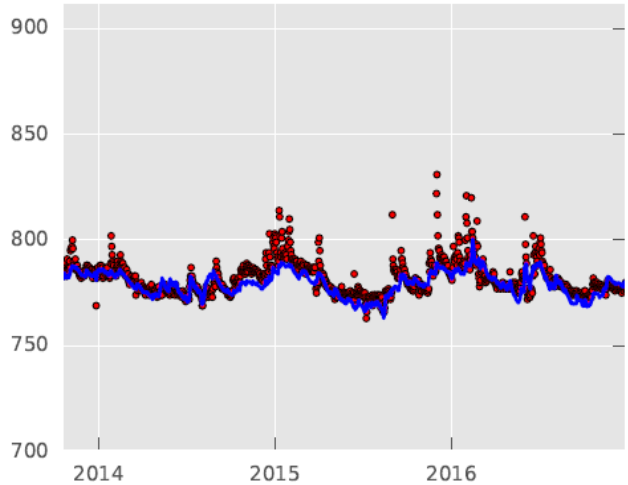

Figure 5.23 Calibration of Metran model for piezometer B46A1559001 during normal Meuse water levels.

This Metran model has been used to simulate the groundwater levels after the accident using the same explanatory variables: precipitation, evaporation, and Meuse water level (*Figure 5.24*).

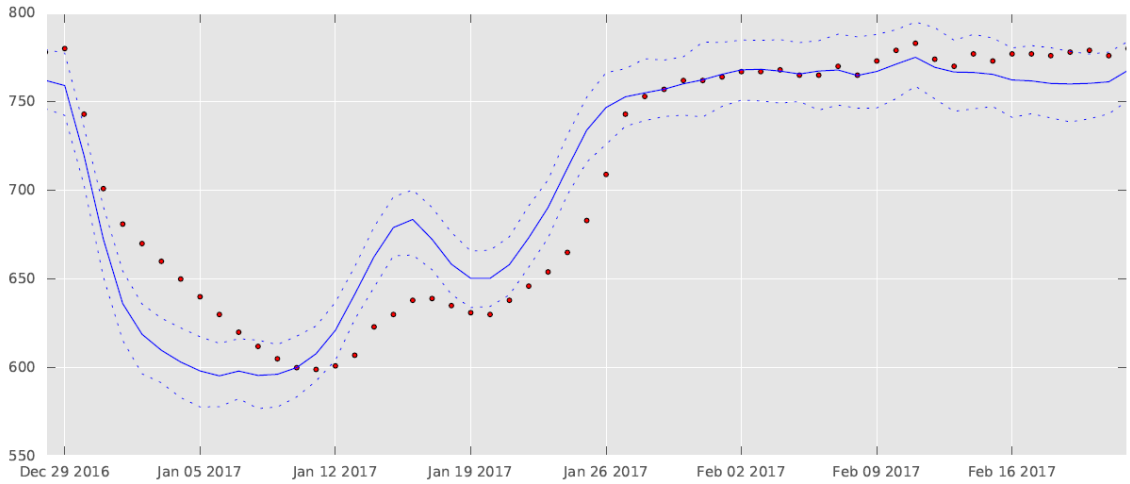

Figure 5.24 Simulation of Metran model (in blue; with 10- and 90-percentile as dotted lines) for piezometer B46A1559001 during unusual change of Meuse water levels (measurements in brown dots).

For this situation, Metran does not simulate the proper timing of the decline and the shape of the recovery also differs ostentatiously. One cause of these deviations is the fact that the

situation is outside the range of groundwater heads and river levels in the calibration period. Another reason is that the response to these extreme river levels is different from the normal response. This may be due to non-linearities and hysteresis in the groundwater system.
This deficiency of the model is illustrated by the fact that the measurements (brown dots in *Figure 5.24*) lie outside the confidence interval created by the stochastic part of the model (the dotted blue lines in *Figure 5.24* represent the 10- and 90-percentile of the simulation).

5.2.2 Climate change scenario results

5.2.2.1 Integrated hydrological model

The effect of the climate scenarios on the groundwater recharge as calculated by the regional model of pilot area De Raam is shown in *Figure 5.25*. No further results are presented in this Subsubsection, but comparisons of De Raam with NHI-LHM are discussed in subsection 6.4.1.

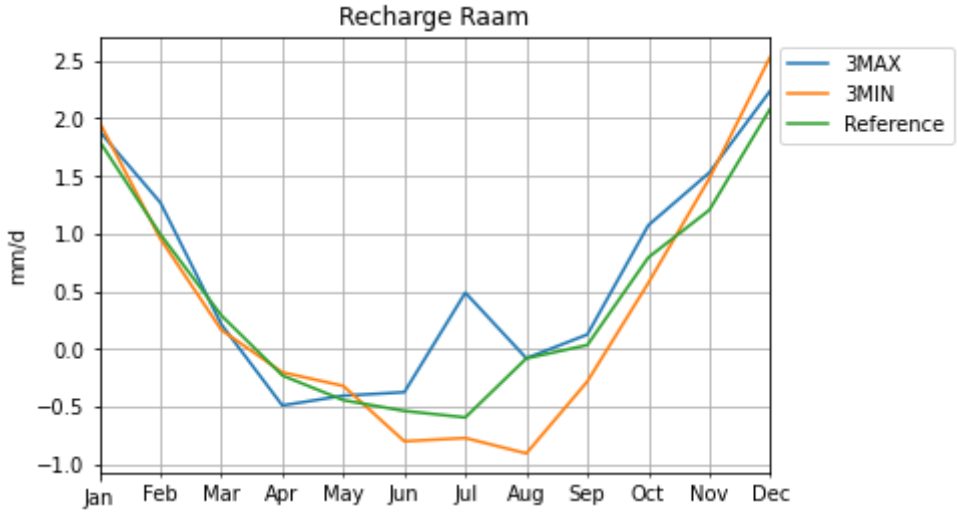

Figure 5.25. Average groundwater recharge as calculated by the regional model of De Raam per month (mm/d) in the period 2011-2018 for the reference situation and the 3 min and 3 max climate scenarios

5.2.2.2 Time series models

The Metran models for the selected piezometers from subsubsection 5.2.1.2 have been used for simulations of the climate change scenarios. The precipitation and evaporation series of the Volkel weather station of the Royal Dutch Meteorological Institute KNMI have been changed using the local change factors for the area of de Raam (see section 4.4).

6 DISCUSSION

6.1 NHI-LHM

The average effective precipitation and average groundwater recharge per month is shown in *Figure 6.1*. These graphs show the average value of the whole country, as an average for every month in the period 2011-2018. Clearly, there is a difference between the effective precipitation and the actual groundwater recharge. The effective precipitation has a much stronger variation throughout the year compared to the groundwater recharge. These differences can be explained by the fact that the actual evaporation is often lower than the potential evaporation and because a part of the precipitation will flow away as surface runoff.

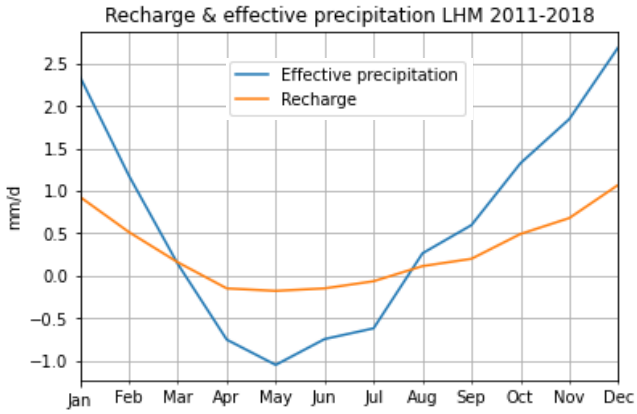

Figure 6.1. Monthly average of effective precipitation and recharge in mm/d

Including an atmosphere-plant model like WOFOST in an integrated model improves the estimation of the actual evapotranspiration. Moreover, the effect of higher CO_2 concentrations on the crop growth can be taken into account, in addition to the change in temperature. Depending on the schematization of the atmosphere-plant model, additional meteorological (and crop) information is needed as input, e.g. WOFOST is based on Penman-Monteith needing daily mean temperature, wind speed, relative humidity, and solar radiation as meteorological input. Because these were not available for the TACTIC climate scenarios, these were simulated without WOFOST.

The use of WOFOST can have a large impact on the model results. For example, a comparison of evapotranspiration in 2003 as modelled with or without WOFOST can result in a change up to 50 mm/year. This influences the calculated groundwater heads; in a relatively dry year they might increase up to 0.25 m compared to a run without WOFOST (Hunink et al., 2019).

The groundwater recharge in urban areas is not well known (Witte et al., 2019). The presence of buildings and pavement has a strong influence on the routing and infiltration of precipitation, with often a large portion going directly into storm sewers or surface water. Also, leaking sewers and drinking water infrastructure can have a large influence (e.g. Foster et al., 1998). In the Netherlands, urbanisation generally leads to a reduction of groundwater recharge because of

the implementation of drainage and the fact that in most urban areas, sewers start to act as drains when they age (Witte et al., 2019). The change of groundwater levels in urban areas may have high financial risks due to flooding, moisture problems (also a health risk), subsidence and deterioration of foundations.

6.2 De Raam

The model for De Raam has been created specifically to support the waterboard in their regional water management. This includes evaluation of local measures to improve the water availability during dry periods. Therefore, a resolution was used that allows for modelling at the parcel scale.

So far, changes in extreme precipitation have not been taken into account in the analysis of climate scenarios for GeoERA. If precipitation intensity changes due to the climate scenarios, an extension of the rapid discharge components might become important, as demonstrated within the Raam pilot.

Within the Lumbricus program in the Netherlands, the software of the regional groundwater model of De Raam has been coupled to a detailed hydraulic surface water model, D-FLOW FM (1D and 2D), through which fluxes between the various model components are dynamically exchanged on an hourly time step basis. This allows the calculation of refined interaction between groundwater and regional surface waters, which especially might be important for extreme rainfall events. The developments with this coupled software will be continued in 2021, especially the tuning of the different model parameters so that the linked models better match the measurements for groundwater and surface waters.

The interim results of the pilot De Raam (for the small river de Hooge Raam) demonstrates that inclusion of detailed processes of surface runoff (encountered in the 2D model, see *Figure 6.2*) and detailed hydraulic 1D calculations (*Figure 6.3*) affects the calculation results of the groundwater calculations. This development might be important for analyzing the effect of climate change on groundwater, if precipitation intensity might increase in the future.

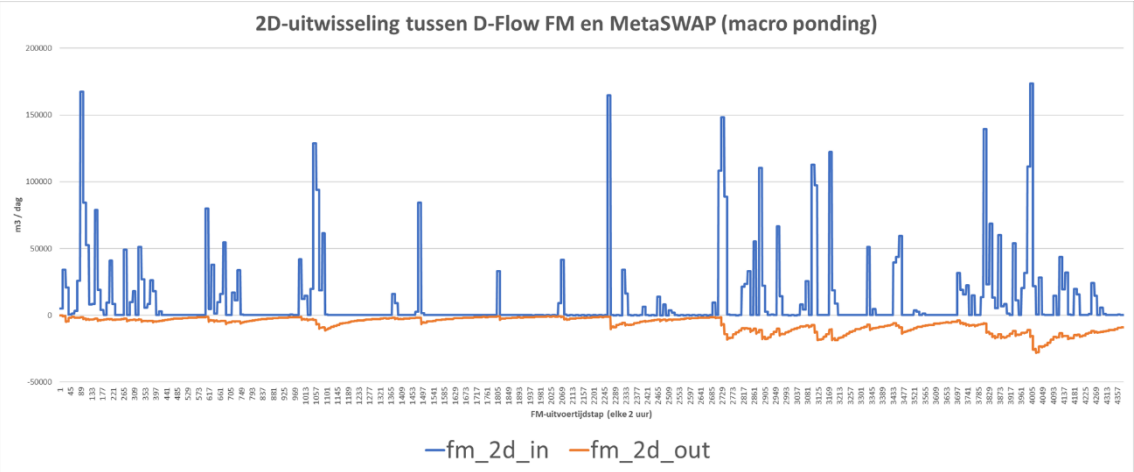

Figure 6.2 Example of exchanges of fluxes between the detailed 2D overland flow (in D-FLOW FM) and the coupled model for the unsaturated zone (MetaSWAP-MODFLOW). Blue: inflow D-FLOW FM, orange: outflow D-FLOW FM.

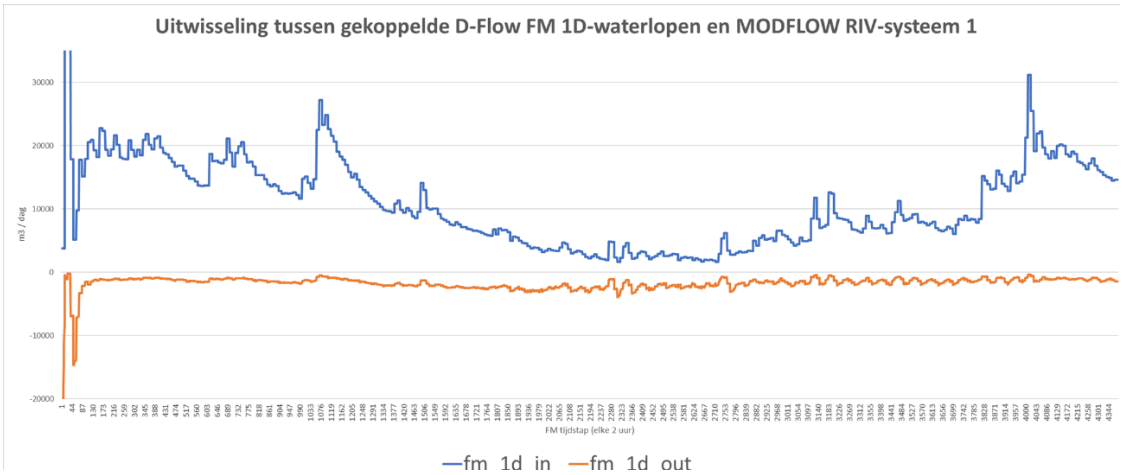

Figure 6.3 Example of exchanges of fluxes between the 1D hydraulic model (D-FLOW FM) and the river systems in the MODFLOW, as a result of the coupled software applied for the Raam region. In blue: inflow D-FLOW FM, orange: outflow MODFLOW.

The accident at the weir of Grave in December 2016 leading to exceptionally low water levels in the River Meuse for the first weeks of 2017 may provide a good opportunity to test the physically based model outside the normal situation it has been calibrated. Although the direct practical purpose may seem limited, it would provide insight into the performance outside of the calibration range. A potentially important aspect would be the release of water from storage and the subsequent refilling of the storage and the hysteresis that may be expected. The accident might provide a future test case for the coupled models of surface water and groundwater.

6.3 Metran

The physical basis of the transfer-noise modelling of time series is limited. The main aspects are the choice of explanatory variables and the shape of the response function. Metran uses an incomplete gamma function, which is connected to a physical schematization (Besbes & de Marsily, 1984).

Also, the output can illuminate physical patterns. The median response time of the groundwater head to precipitation has a similar pattern as the distance between surface waters and surface elevation (*Figure 6.4*).

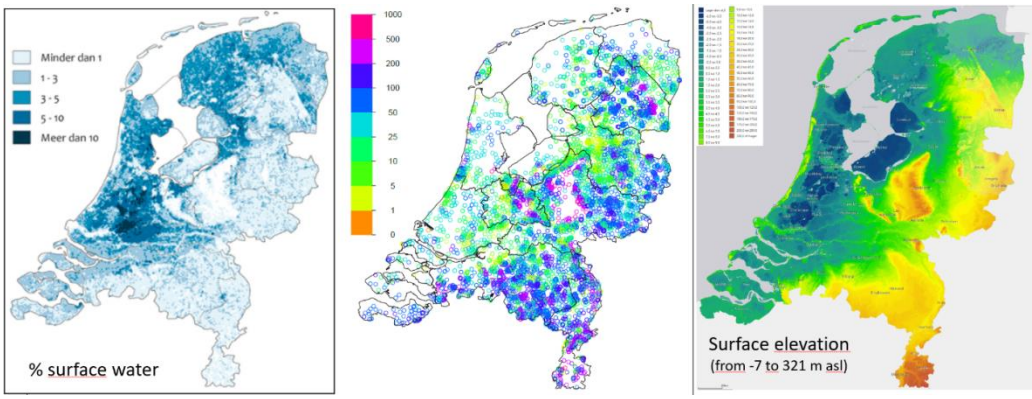

Figure 6.4 Precipitation response time [days] (centre, Figure 5.7), surface percentage of surface water (left) and surface elevation (right)

Comparison of *Figure 5.6* with *Figure 6.4* or *Figure 5.7* shows that the total response also has a similar pattern. However, the correlation between both quantities decreases for larger values (*Figure 6.5*).

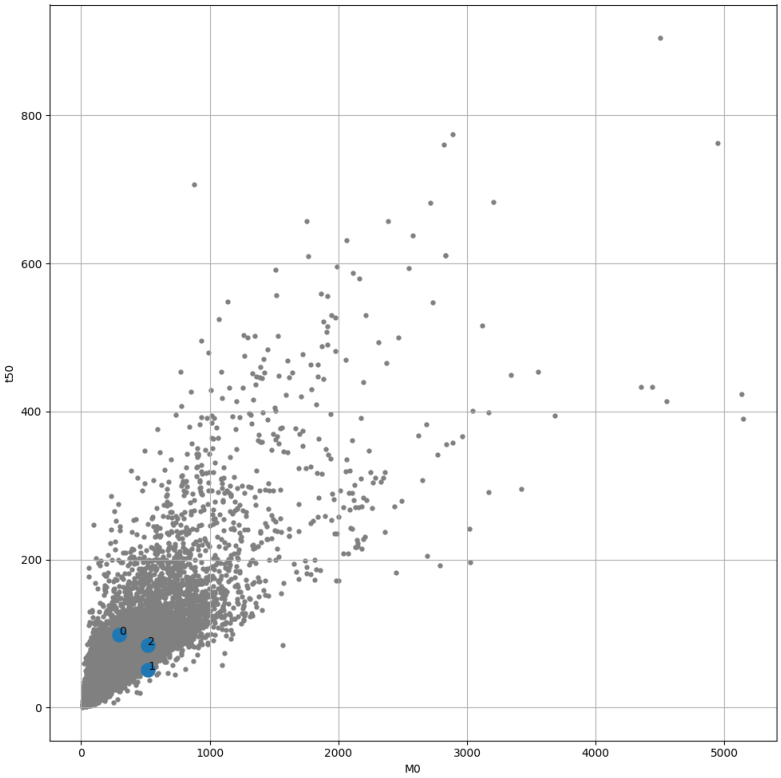

Figure 6.5 Mean precipitation response time t50 [days] as function of the total precipitation response M0 [cm per m/d] for all good time series models together with K-means cluster centers for the upper regional aquifer (WVP2 in NHI-LHM).

The connection between these characteristics of the precipitation response and the physical properties of the groundwater system is not well known and is topic of research (e.g. Haaf et al., 2020). Here, K-means clustering (Pedregosa et al., 2011) has been used to obtain insight in the variation of ratio between the total precipitation response M0 and the mean precipitation response time t50 in *Figure 6.5*. The time series models of Cluster 2 have an average ratio of M0 and t50. The response time is relatively high in cluster 0 and relatively low in cluster 1.

The map in *Figure 6.6* shows the clusters for piezometers in the upper regional aquifer. The Western part of the Netherlands contains mostly cluster 0. This mainly is relatively low lying polder area where the upper regional aquifer is covered by a Holocene confining layer. In the higher areas without a confining layer, the clusters 1 and 2 are interspersed.

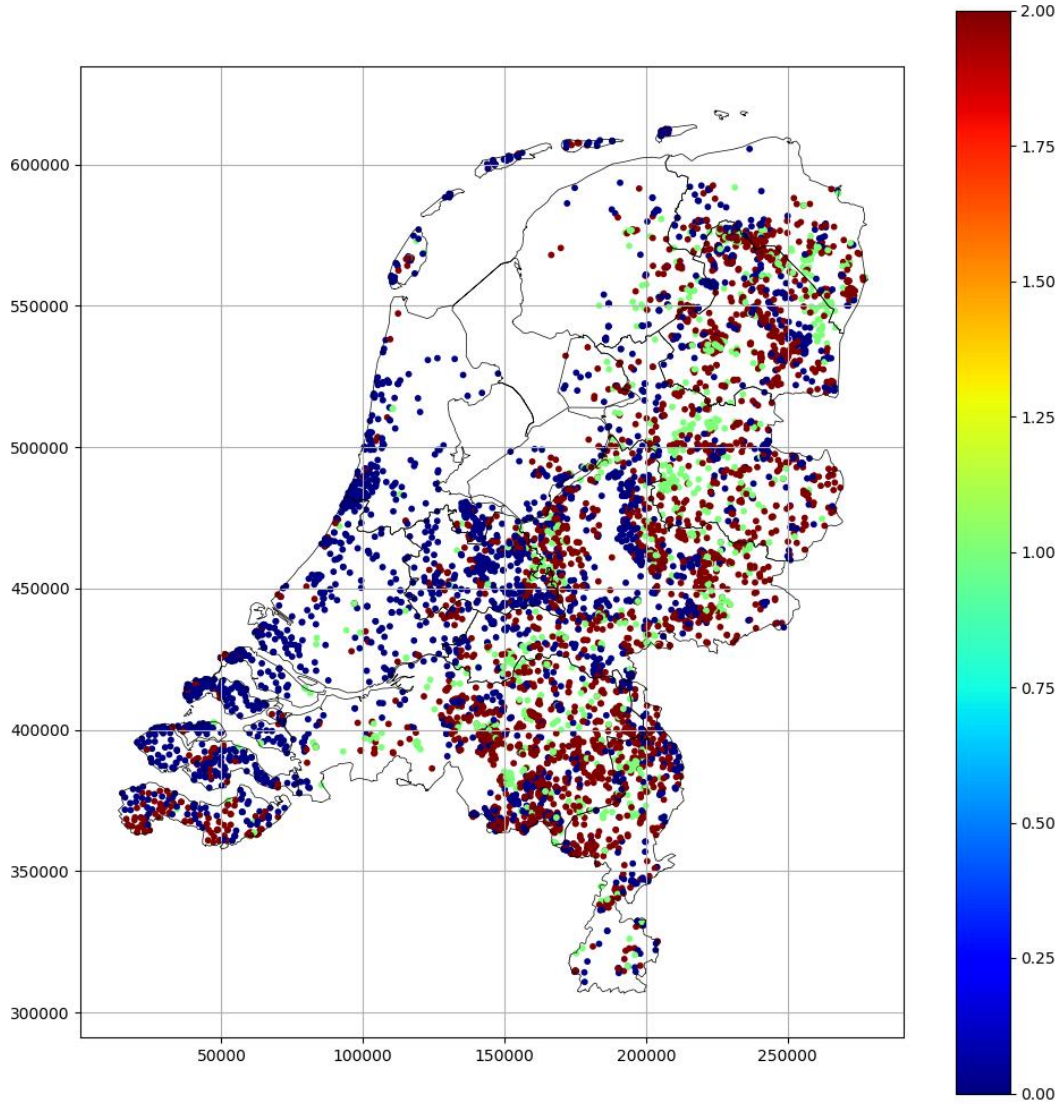

Figure 6.6 K-means clusters for the total precipitation response M0 (relative to the average M0) and ratio of M0 over the median response time t50 for the upper regional aquifer (WVP2 in NHI-LHM).

The piezometers selected for the regional pilot (subsubsection 5.2.1.2 have been simulated with Metran and the results are compared with heads from the national model NHI-LHM in section 6.3.

6.4 Comparison between models

6.4.1 Regional and national physically based distributed models

Figure 6.7 shows the difference between the effective precipitation for the national model and regional model. This figure illustrates that there are differences following from the way the meteorology has been created, using only data from weather and precipitation stations for the national model, but also radar information for De Raam. Also, the discretisation was different. The differences are small. The effective precipitation for the Raam model is about 3.5 mm/year higher than the effective precipitation of the national model, which is about 100 mm/year.

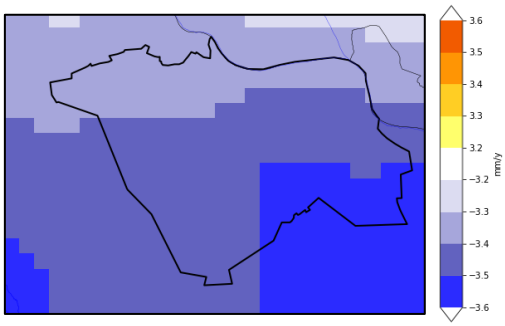

Figure 6.7. The difference between the effective precipitation of the LHM and De Raam model (mm/year). Calculated as LHM minus De Raam.

Figure 6.8 shows the depth of the phreatic groundwater table below the surface for both model for the three degrees climate scenarios.

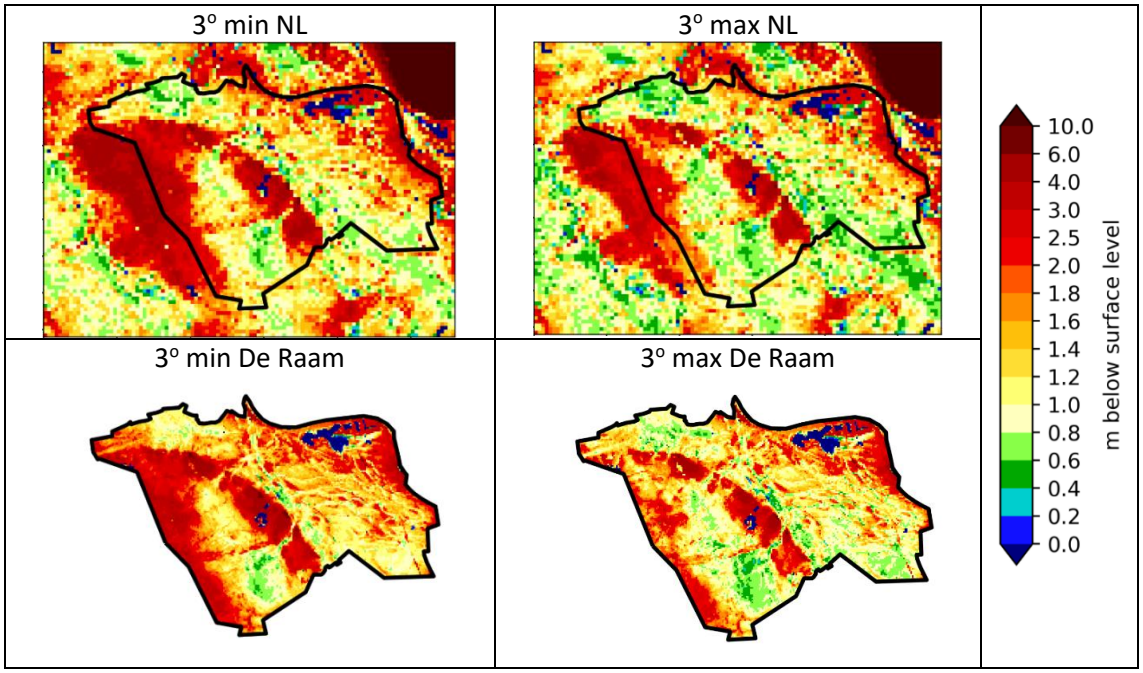

Figure 6.8. Phreatic head in m below surface level for the 3 min (left) and 3 max scenario (right). The top row are the results from the national model, the bottom row are the results of the local model of De Raam.

The phreatic head distribution of both models (see *Figure 6.8*) are similar, although there are some differences. The phreatic heads according to the regional model of De Raam are slightly lower compared to the national model, meaning that they are further below surface level. Moreover, due to the fine grid size of the regional model, a much more detailed head distribution can be distinguished.

The average groundwater recharge as computed by the national and regional model is spatially compared in *Figure 6.10*. In *Figure 6.9* the average groundwater recharge in the whole area for every month is plotted. Both figures clearly indicate that the groundwater recharge according to the regional model is lower, at some points up to 200 mm/year. This corresponds to the differences that were seen in the results of the phreatic head, where it was shown that the phreatic heads according to the regional model are lower. This shows that the coarse resolution of the national model attenuates the effect of climate change.

In *Figure 6.11*, the recharge of the simulations with the 3° min and 3° max scenarios for the regional model and national model are compared to their reference situations. These figures show that the effect of the climate scenarios is slightly different for both models. Especially for the 3° max scenario: some regions that have a relatively large increase in recharge (at the west boundary) according to the national model, have a relatively low increase according to the regional model.

The variation of the groundwater recharge during the year as calculated by the regional model (see *Figure 5.25*) and for the national model (see *Figure 5.14*) also compare quite well.
Spatially the differences are more distinct, as can be seen in *Figure 6.10* and *Figure 6.11*.

In general, it can be concluded that the finer grid size for the regional model results in a much more detailed image of the effect of climate change in the pilot area. The national model results are only useful to describe a general effect of climate change in the area. Due to the fine grid size of the regional model, also the regional differences within the pilot area become known.

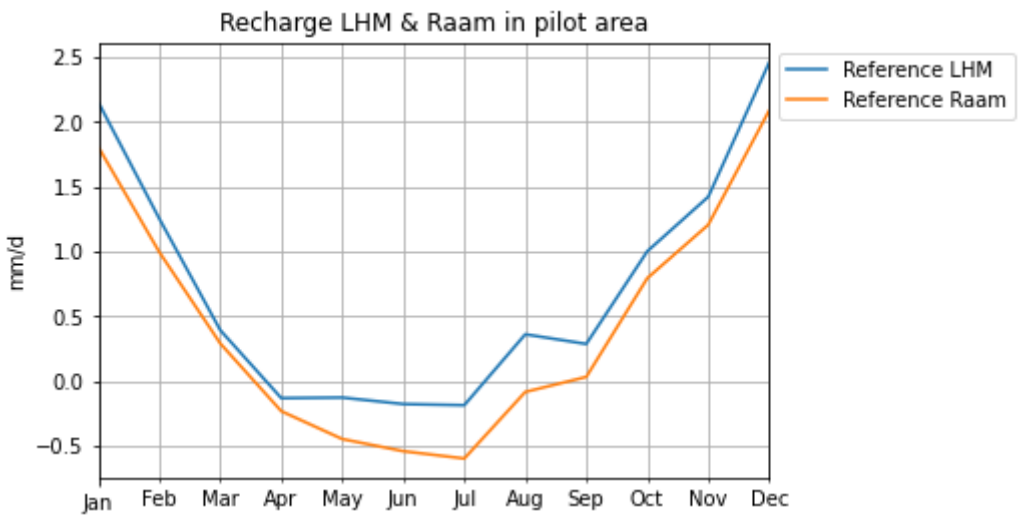

Figure 6.9. Average monthly recharge in the period 2011-2018 in pilot area De Raam as calculated by the national model (LHM, blue) and regional model (Raam, orange)

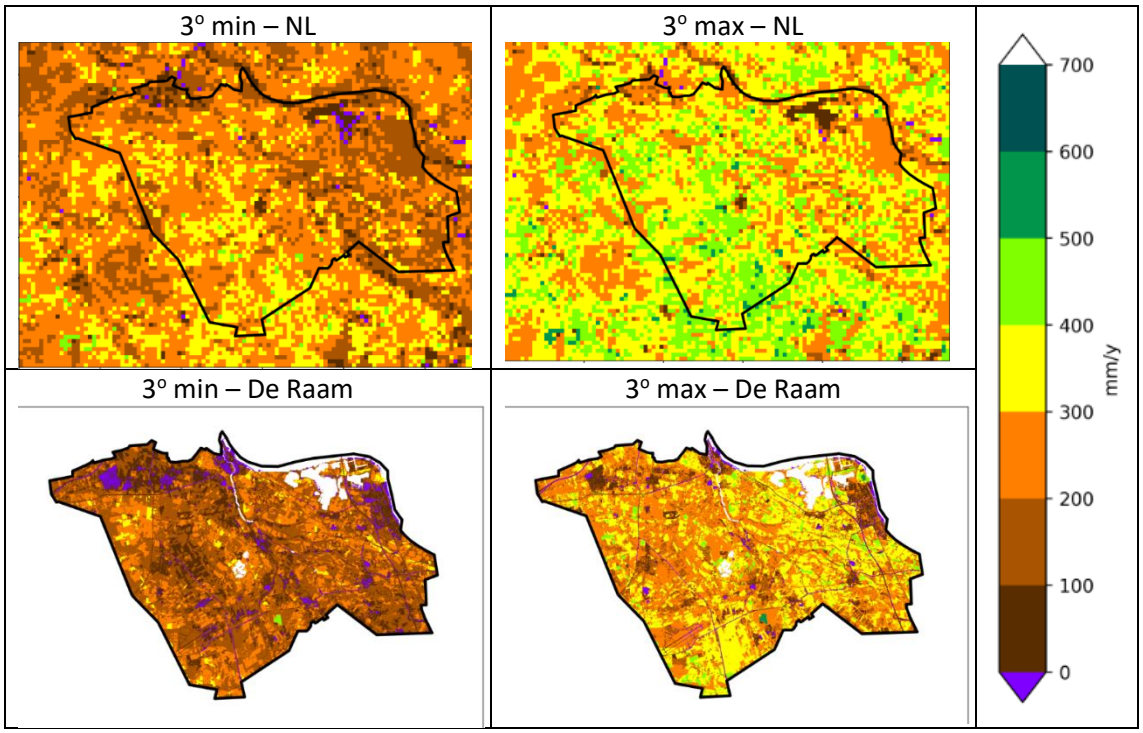

Figure 6.10. Groundwater recharge in mm/year for the 3° min scenario (left) and 3° max scenario (right). The top row are the results from the national model, the bottom row are the results of the regional model of De Raam

3° min – NL	3° max – NL	

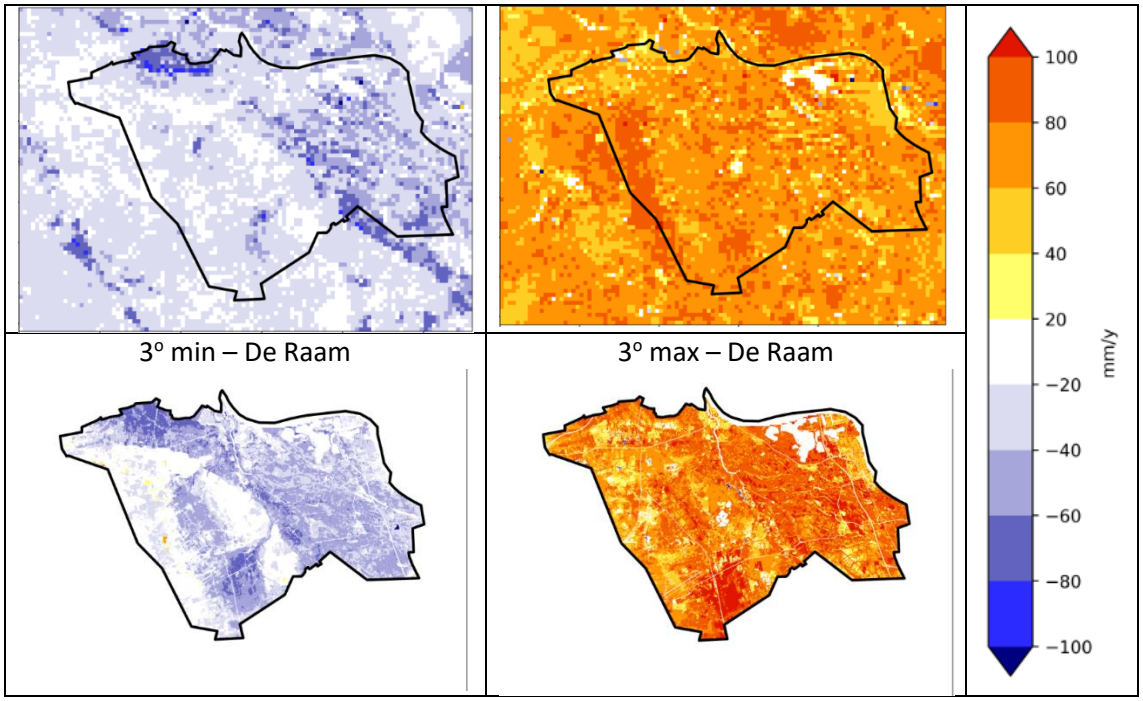

Figure 6.11. Groundwater recharge change in mm/year compared to the reference situation of the national model (top) and regional model (bottom) for the 3° min (left) and 3° max (right) scenario.

6.4.2 Physically based distributed models and time series models

The physically based distributed models NHI-LHM and de Raam have been built up from a conceptual model of the hydrology and the subsurface together with a parametrization derived from the knowledge of this physical system. The Metran models have a very limited physical base: the use of the incomplete gamma function as transfer function (Besbes & de Marsily, 1984) and the selection of explaining variables. This leads to differences in the results.

6.4.2.1 Reference situation

Figure 6.12 shows the measurements of the first piezometer of monitoring well B45B0174, which is located about 10 meters below the surface of 13.62 meters (from 3.51 to 1.5 m NAP).

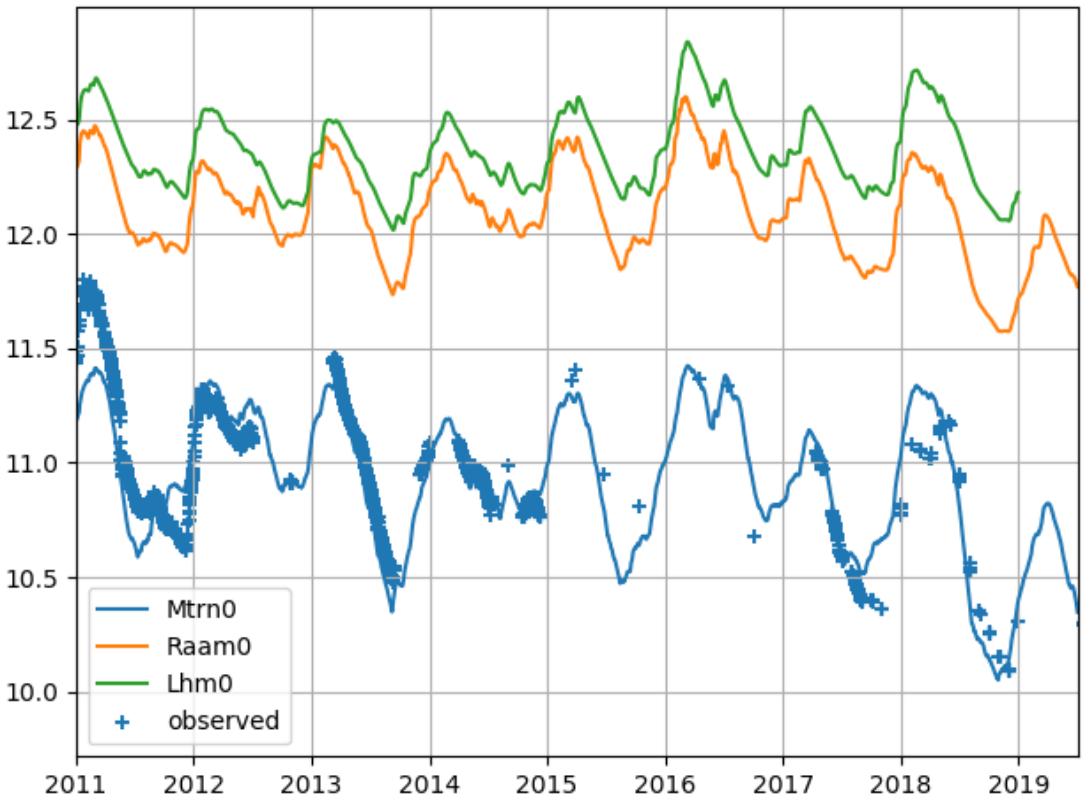

Figure 6.12 Measured groundwater heads for B45F0174001 together with simulated values from Metran (Mtrn0), de Raam model (Raam0), and NHI-LHM (Lhm0).

The main difference between the modelled heads in *Figure 6.12* is the average level. That of the Metran model corresponds well with the measurements. A deviation is to be expected for the distributed models because of the spatial discretization, which leads to representative values of cells of 250 m x 250 m and 25 m x 25 m for the national and the regional model respectively. In these models the recharge processes depend on the depth of the groundwater below the surface. The difference between the actual surface elevation and the model value is 1.35 meter for the national model and 0.23 m for the regional model (see Table 6-1). This corresponds to the difference in averages of the model heads in *Figure 6.12* for the National model. So, the surface processes may be simulated adequately, despite the deviation from the heads measured at this specific point.

Table 6-1 surface elevation from metadata of piezometer and models (m NAP).

Location	surface	NHI-LHM	De Raam
B45F0174	13.62	14.97	13.85
B45F0279	20.51	20.77	20.83
B46C0478	17.16	17.53	17.71

The fluctuation of all three models is less than the measured fluctuation of the groundwater heads in *Figure 6.12*, especially in the first three years of the graph. The drop of the head in the dry summer of 2018 is simulated better by Metran than the distributed models.

Figure 6.13 shows a similar graph for the upper piezometer of monitoring well B46C0478. The piezometer is perforated between 13.19 and 11.19 m NAP, while the surface elevation here is 17.16 m NAP.

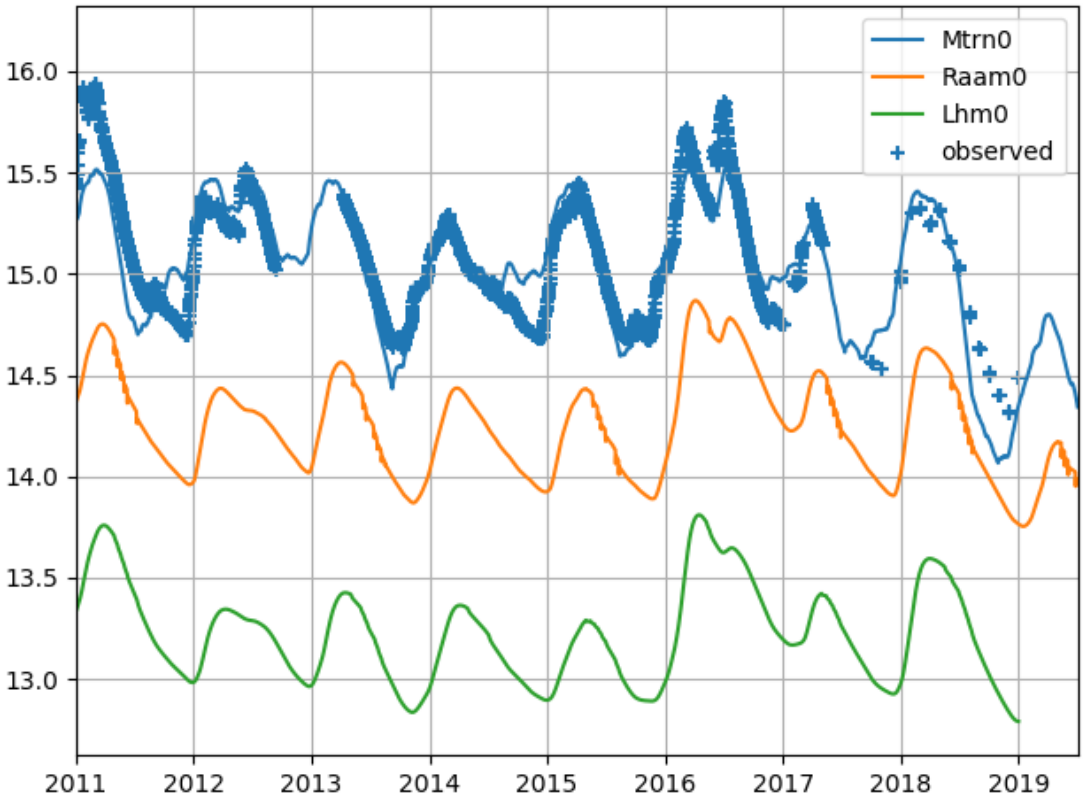

Figure 6.13 Measured groundwater heads for B46C0478001 together with simulated values from Metran, de Raam model, and NHI-LHM.

Figure 6.13 also shows a systematic difference between the models. Now the heads from the distributed models are lower, while the surface elevation is again higher (see Table 6-1). The regional model de Raam matches the measured heads much better than the national model. The distributed models simulated the fluctuation of the heads better for the year 2011. Metran overestimates the drop of the heads in 2018 and the minimum is off in timing. The distributed models underestimate the drop slightly, and model the timing better than Metran. This could be due to non-linear behaviour that the physically based models can reproduce, while the Metran model is linear.

6.4.2.2 Climate change scenarios

Figure 6.14 and *Figure 6.15* show comparisons for integrated model results with time series models simulations for climate change scenarios in the upper piezometer of two monitoring wells.

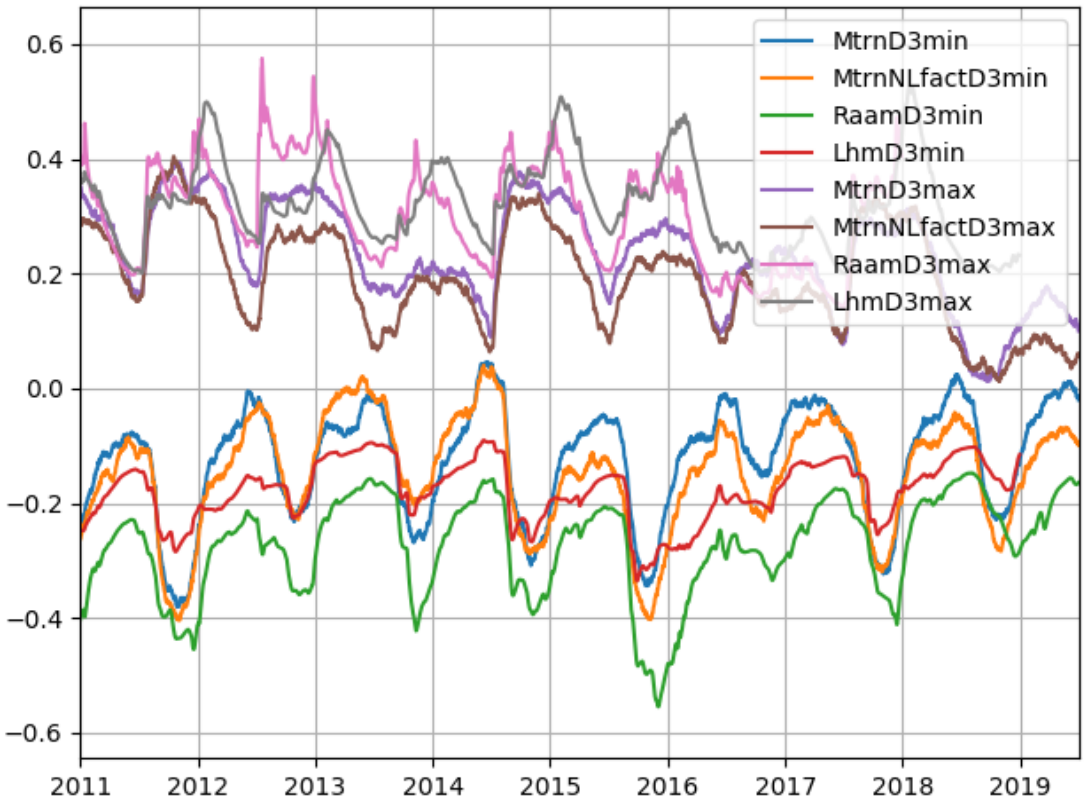

Figure 6.14 Calculated changes for the 3min and 3max climate change scenarios with respect to the reference simulation for piezometer B45F0174001.

There is some impact of the change factors visible in the two Metran simulations (Mtrn with De Raam factors, and MtrnNLfact with national factors). The difference in change factors is also contained in the integrated models. Moreover, the simulations for De Raam seem to benefit from the more detailed regional model.

The physical relations in the integrated models create different dynamics of the groundwater table than the relatively simple extrapolation of the current situation in the time series models. Because of this the changes from the integrated models are probably more reliable than from the time series models. However, given the larger deviation from the measurements for the current situation, the absolute values should be used with care.

This probably can be improved by constructing more accurate maps of the reference groundwater head by combining the measurements or time series models together with the integrated model results. This can be done by kriging with model output as a trend surface (e.g. Zaadnoordijk et al., 2021). The changes simulated by the integrated model are subsequently superimposed on this reference head map.

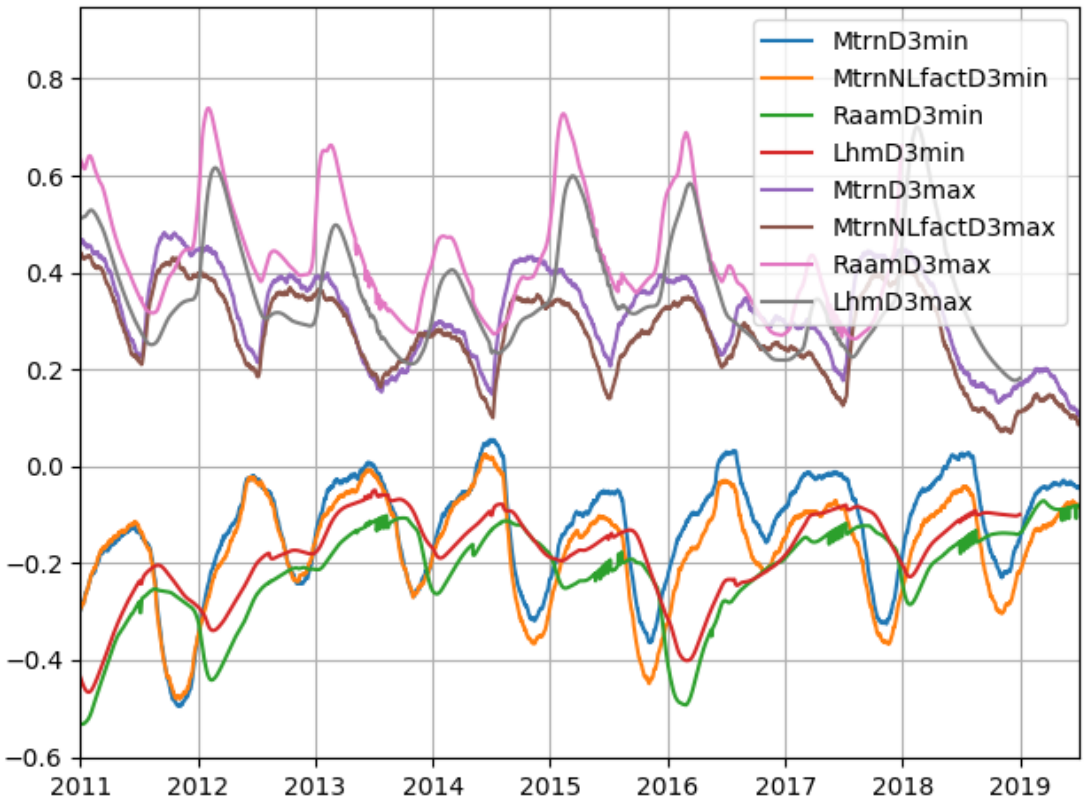

Figure 6.15 Calculated changes for the 3min and 3max climate change scenarios with respect to the reference simulation for B46C0478001.

The fact that simulations with time series models assume that the groundwater system does not change (and in case of the Metran simulations presented also assumes a linear behaviour) does limit their usefulness for propagation of climate change in the groundwater system, compared to the integrated models. On the other hand, making separate time series models for different periods is an easier way to detect whether the groundwater system has changed or temporarily behaves differently.

7 CONCLUDING REMARKS

Two pilots in the Netherlands have been investigated using integrated physically-based distributed hydrological modelling and transfer-noise time series modelling. The national pilot and the regional pilot De Raam have a large difference in resolution (250 m x 250 m and 25 m x 25 m, respectively), related to the different purposes. The national model is used for the management of the main rivers and for national policy development. The model for De Raam is intended for improving the regional water management, e.g. by evaluating concrete local measures.

A comparison of the results of the national and regional pilot has indicated that the finer resolution is necessary to study local variations within the pilot area. The national model is only able to roughly describe the effect of climate change in the pilot area. Moreover, the effect of climate change according to a regional model is also slightly more profound compared to the national model.

The time series modelling provides information only at locations of monitoring wells, although it is possible to create spatial images of various outputs.

The time series models provide more accurate history matching at the well locations, while the integrated models are better predictors for future scenarios.

The recharge calculated by the integrated models is more reliable than that of time series models calibrated only on groundwater heads. The time series model allows for an estimation of the correlation of the groundwater levels with surface water levels, which provides a limited insight in the groundwater-surface water interaction compared to the integrated models.

Both types of models can simulate climate change scenarios, albeit results of the integrated models are much more trustworthy, provided the important processes are included with an adequate parametrisation. It can be useful for climate analysis to further detail the processes within the integrated models, for example coupling with detailed crop models if crop evaporation might change in the future situation, or with detailed surface water models if the intensity of precipitation changes significantly.

The effort to setup and maintain the integrated model is much larger than for time series modelling. Combined use provides extra benefits e.g. improved spatial continuous history matching, determining important processes to include in the integrated model by time series modelling with known influences, and selection (and weighing) of piezometers to use for calibration.

8 REFERENCES

AHN2 (2013) accessed at 11-01-2019 through http://www.ahn.nl/

Berendrecht, W.L., F.C. van Geer (2016) A dynamic factor modeling framework for analyzing multiple groundwater head series simultaneously, Journal of Hydrology, volume 536, pages 50-60, http://dx.doi.org/10.1016/j.jhydrol.2016.02.028

Berendrecht, W.L. (2021, in prep.). Validatie en toetsing LHM 4.1. Deelrapport 1: grondwater, Berendrecht Consultancy, Harderwijk, Netherlands.

Besbes, M, G. de Marsily (1984) From Infiltration to Recharge: use of a parametric transfer function, Journal of Hydrology, volume 74, pages 271-293.

Besselink, D. (2018) Integrated plan development De Raam (in Dutch: Gebiedsplan Raam). Arcadis report C03091.000256.0220, Arcadis, Arnhem, Netherlands. https://www.aaenmaas.nl/publish/pages/734/gebiedsplan_raam_-_september_2018.pdf

Bos-Burgering, L. & J. Hunink (2020) Optimalisatie grondwatermodel instrumentarium Waterschap Aa en Maas (Optimizing the groundwater modelling instrument of water board Aa and Maas; in Dutch). Deltares report 1220765-020, Delft

Bot, B. (2016) Grondwaterzakboekje GWZ2016. Bot Raadgevend Ingenieur, Rotterdam, Netherlands.

Delsman, J.R., G.H.P., S. Huizer (2021, in prep) Salinity modeling in the national groundwater model of the Netherlands Hydrological Instrument, Deltares, Utrecht, the Netherlands.

De Lange, W.J. (1991) NAGROM, een landsdekkend instrument voor grondwaterbeleid en -beheer (NAGROM a nationwide instrument for groundwater policy and management; in Dutch), H2O, volume 24, no. 16, pages 450-455.

De Lange, W.J., G.F. Prinsen, J.C. Hoogewoud, A.A. Veldhuizen, J. Verkaik, G.H.P. Oude Essink, P.E.V. van Walsum, J.R. Delsman, J.C. Hunink, H.Th.L. Massop, T. Kroon (2014) An operational, multi-scale, multi-model system for consensus-based, integrated water management and policy analysis: The Netherlands Hydrological Instrument, Environmental Modelling & Software (59), 98-108, http://dx.doi.org/10.1016/j.envsoft.2014.05.009.

Doherty, J., 2015. Calibration and Uncertainty Analysis for Complex Environmental Models. Watermark Numerical Computing, Brisbane, Australia. ISBN: 978-0-9943786-0-6 (see https://pesthomepage.org/).

Foster, S.S.D., A. Lawrence, B. Morris (1998) Groundwater in urban development: assessing management needs and formulating policy strategies, World Bank Technical Paper; no. WTP 390, Washington DC, USA. http://documents.worldbank.org/curated/en/380261468765030397/Groundwater-in-urban-development-assessing-management-needs-and-formulating-policy-strategies390.

Haaf, E., M. Giese, B. Heudorfer, K. Stahl, R. Barthel (2020) Physiographic and climatic controls on regional groundwater dynamics. Water Resources Research, volume 56, e2019WR026545. https://doi.org/10.1029/2019WR026545.

Hughes, J.D., M.J. Russcher, C.D. Langevin, R. R. McDonald, & E. D. Morway (2021, in prep) The MODFLOW 6 Application Programming Interface for simulation control and software interoperability. USGS report

Iwaco (1992) Onderzoek grondwaterbeheer Midden Nederland (GMN): Modellering watersysteem (Investigation groundwater management Central Netherlands (GMN): modelling watersystem; in Dutch). Iwaco consultants for water and environment, Rotterdam, the Netherlands, Juli 1992.

Janssen, G., J. Hunink, T. Kroon, J. Pouwels, I. America, J. Verkaik, G. Prinsen, E. Schoonderwoerd P. van Walsum and A. Veldhuizen (2021, in prep) A Nationwide Integrated Hydrological Model for National Policy Support

Klopstra, D., W. Berendrecht, M. Pezij, V. van der Vliet, A. van Doorn en J. Velstra (2021, in prep) Validatie LHM, samenvattend hoofdrapport (Validation LHM, summary main report; in Dutch). HKV report

Kroes, J.G., J.C. van Dam, R.P. Bartholomeus, P. Groenendijk, M. Heinen, R.F.A. Hendriks, H.M. Mulder, I. Supit, P.E.V. van Walsum (2017) SWAP version 4; Theory description and user manual. Wageningen, Wageningen Environmental Research, Report 2780.

Hunink, J.C., P.E.V. van Walsum, P.T.M. Vermeulen, J.R. Pouwels, H.P. Bootsma, G.M.C.M. Janssen, W. Swierstra, G.F. Prinsen, A. Meshgi, A.A. Veldhuizen, W.J. de Lange, J. Hummelman, L.M.T. Bos-Burgering en T. Kroon (2019) Veranderingsrapportage LHM 4.0; Actualisatie van het lagenmodel, het topsysteem en de bodem-plant relaties (Change report LHM 4.0; Actualisation of the subsurface schematisation, the topsysteem and soil-plant relations; in Dutch), Deltares report 11203718-000-BGS-0001

Janssen, G.M.C.M., P.E.V. van Walsum, I. America, J.R. Pouwels, J.C. Hunink, P.T.M. Vermeulen, A. Meshgi, G.F. Prinsen, N. Mulder, M. Visser en T. Kroon. Veranderingsrapportage LHM 4.1; Actualisatie van het lagenmodel, het topsysteem en de bodemplant relaties. Deltares rapport 11205261-000-BGS-0001, 2020

Klein Tank, A., J. Beersma, J. Bessembinder, B. Van den Hurk, G. Lenderink, G. (2014). KNMI'14: Climate Change scenarios for the 21st Century–A Netherlands perspective. Report, KNMI, de Bilt, Netherlands. http://www. climatescenarios.nl

KNMI (2011) Klimaatatlas, accessed at 10-01-2019 through http://www.klimaatatlas.nl/.

Kroon, T., A.A. Veldhuizen, L.M.T. Burgering, P.E.V. van Walsum, G. Janssen, F.J.E. van der Bolt, J. Verkaik (2017) Improvements National Hydrological Model NHI-LHM: preparation for water

quality simulation (in Dutch: Veranderingsrapportage LHM 3.3.0; ontwikkelingen ten behoeve van de waterkwaliteit. Deltares report 11200573-000-BGS-0001, Deltares, Utrecht, Netherlands.

Lieste, R., K. Kovar, J.G.W. Verlouw, J.B.S. Gan (1993) Development of the GIS-based "RIVM National Groundwater Model for The Netherlands (LGM)" In: Application of Geographic Information Systems in Hydrology and Water Resources (ed. by K. Kovar & H. P. Nachtnebel) (Proc. Int. Conf. HydroGIS'93, Vienna, April 1993), IAHS Publication No. 211, pages 641-651.

NHI dataportal (2019) Water distribution network of the national hydrological model, accessed at 11-01-2019 through https://data.nhi.nu/.

Obergfell, C., M. Bakker, K. Maas (2019). Estimation of average diffuse aquifer recharge using time series modeling of groundwater heads. Water Resources Research, Volume 55. https://doi.org/10.1029/2018WR024235.

Prinsen, G., F. Sperna Weiland and E. Ruijgh (2015). The Delta Model for Fresh Water Policy Analysis in the Netherlands. Water Resour Manage 29:645–661.

Sperna Weiland, F., B. van der Hurk, T. Kroon, E. Schoonderwoerd (2021, in prep.) Consistent projections of European scale future hydrological change for 1 and 3 degrees warming scenarios, to be submitted.

TNO-GSN (2021a) REGIS II: the hydrogeological model, TNO Geological Survey of the Netherlands, Utrecht, https://www.dinoloket.nl/en/regis-ii-hydrogeological-model.

TNO-GSN (2021b) Detailing the upper layers with GeoTOP, TNO Geological Survey of the Netherlands, Utrecht, https://www.dinoloket.nl/en/detailing-the-upper-layers-with-geotop.

Topografische Dienst Kadaster (2019) Surface water in the Netherlands (in Dutch), accessed at 11-01-2019 through https://www.clo.nl/indicatoren/nl1401-oppervlaktewater-in-nederland.

Van der Gaast, J.W.J., P.J.T. Van Bakel (1997) Differentiation of water cources for pesticides (in Dutch: Differentiatie van waterlopen ten behoeve van bestrijdingsmiddelen in Nederland). Rapport 526, SC-DLO. Wageningen, Netherlands.

Vermeulen, P.T.M, F.J. Roelofsen, J. Hunink, G.M.C.M. Janssen, B. Romero Verastegui, J. van Engelen & M. Russcher (2020) iMOD 5.1 User Manual. Deltares rapport.

Vewin (2017) Drinkwaterstatistieken 2017. Van bron tot kraan (Drinkwater statistics, from source to tap; in Dutch)

Van Walsum, P. E. V., (2017) SIMGRO V7.3.3.2, Users Guide. Tech. Rep. Alterra-Report 913.2, Alterra, Wageningen. 111 pp.

Van Walsum, P.E.V., and A.A. Veldhuizen (2011). Integration of models using shared state variables: Implementation in the regional hydrologic modelling system SIMGRO. Journal of Hydrology 409 (2011) 363–370.

Witte, J.P.M., W.J. Zaadnoordijk, J.J. Buyse (2019) Forensic Hydrology Reveals Why Groundwater Tables in The Province of Noord Brabant (The Netherlands) Dropped More Than Expected, Water, Volume 11, No. 478, doi:10.3390/w11030478.

Wosten, H, F.de Vries, T. Hoogland, H. Massop, A. Veldhuizen, H. Vroon, J. Wesseling, J. Heijkers, A. Bolman (2012) Bofek2012, new soil physical schematization of the Netherlands (in Dutch: de nieuwe bodemfysische schematisatie van Nederland) Alterra rapport 2387, Alterra, Wageningen, Netherlands. http://edepot.wur.nl/247678

Zaadnoordijk, W.J. (2018) Time series modeling of piezometric heads – determination of precipitation response in the presence of other stresses and hydrogeological heterogeneity, AGU Fall Meeting 2018 - poster H23O-2160, Washington DC, USA, 10-14 December 2018, https://www.essoar.org/doi/abs/10.1002/essoar.10500086.1.

Zaadnoordijk, W.J., A. Lourens (2019) Groundwater dynamics in the aquifers of the Netherlands, TNO report TNO 2019 R12031, TNO Geological Survey of the Netherlands, Utrecht, Netherlands.

Zaadnoordijk, W.J., S.A.R. Bus, A. Lourens, W.L. Berendrecht (2019) Automated Time Series Modeling for Piezometers in the National Database of the Netherlands, Groundwater, volume 57, no. 6, pages 834-843, https://onlinelibrary.wiley.com/doi/epdf/10.1111/gwat.12819, open access.

Zaadnoordijk, W.J., A. Lourens, J.M.M. Hettelaar (2021) Kaarten met grondwaterisohypsen in de provincie Utrecht 2009-2020 (maps with groundwater head contours in the province of Utrecht; in Dutch), commissioned by the Province of Utrecht, report TNO 2021 R10281, TNO-GSN, Utrecht, the Netherlands.